STEVE
(WEBSITE)

Bulletin 504

BUREAU OF MINES

FLUID FLOW THROUGH PACKED AND FLUIDIZED SYSTEMS

By M. Leva, M. Weintraub, M. Grummer, M. Pollchik, and H. H. Storch

UNITED STATES GOVERNMENT PRINTING OFFICE, WASHINGTON : 1951

UNITED STATES DEPARTMENT OF THE INTERIOR

Oscar L. Chapman, Secretary

BUREAU OF MINES

James Boyd, Director

For sale by the Superintendent of Documents, U. S. Government Printing Office
Washington 25, D. C. — Price $1.00

CONTENTS

ILLUSTRATIONS

FLUID FLOW THROUGH PACKED AND FLUIDIZED SYSTEMS[1]

by

M. Leva,[2] M. Weintraub,[2] M. Grummer,[2] M. Pollchik,[2] and H. H. Storch[3]

Introduction

WITH the development of new processes for the production of synthetic liquid fuels, an extensive literature search was undertaken to uncover fundamental relationships between fluid and heat flows and the operating variables of new types of converters. Examination of published correlations revealed that considerable uncertainty existed in the correlation of the operating variables of such equipment with the pressure drops which could be expected through packed and fluidized systems; correlations proposed in the literature differed from each other frequently by as much as 75 to 100 percent. Because new processes, especially more recent modifications of the original Fischer-Tropsch process, must compete with old, firmly established processes on the basis of unit product cost, the pressure-drop correlations in the literature were considered to be too inaccurate for use in calculating the energy required to pass fluids through packed beds.

The following study was begun in 1946 to develop correlations that would be suitable for the design of new equipment in which fluids are brought into contact with granular materials. To arrive at general relationships, systems were chosen that did not involve chemical reactions, and a particular effort was made to give the correlations only in terms of quantities that are ordinarily available from general process and design specifications.

[1] Work on manuscript completed November 28, 1950.

[2] Chemical engineer, Research and Development Branch, Office of Synthetic Liquid Fuels, U. S. Department of the Interior, Bureau of Mines, Bruceton, Pa.

[3] Chief, Research and Development Branch, Office of Synethetic Liquid Fuels, U. S. Department of the Interior, Bureau of Mines, Bruceton, Pa.

ACKNOWLEDGMENTS

The authors are grateful to their associates in the Bureau of Mines for indispensable help during the investigations and construction and assembly of the equipment. They take particular pleasure in acknowledging the interest, cooperation, and constructive suggestions of M. A. Elliott, E. L. Clark, J. H. Crowell, and E. H. Amick, Jr.

Editorial assistance was rendered by Norma Golumbic and R. C. Grass.

Construction details pertaining to the various units were supervised by W. E. Miller, W. H. Williams, and W. L. Fauth. The graphs were made by C. R. Siple and J. J. Vidosh, and the reproductions by G. L. Henneman of the Graphic Services Section.

The authors are grateful also for the general assistance given by W. T. Reed and J. P. Stein, of the Coal Research Section, and to J. Field, of the Gas Synthesis Section, for making available some data on flow of oils through catalyst powders.

The authors want to thank A. O. Oman and K. M. Watson, of the University of Wisconsin, for having supplied typical pieces of packing materials for examination of surface roughness; Chemical Engineering Progress for permission to copy various figures and parts of the text published previously; and Inez G. Booher, Myrtle R. Lee, and Sophie Radosevich for typing the manuscript.

LITERATURE SURVEY

FLUID FLOW THROUGH PACKED BEDS

Studies of fluid flow through beds of solids have been reported in such diversified journals as those in the fields of petroleum production, sanitary engineering, chemical engineering, physics, hydrodynamics, mechanical engineering, physical chemistry, and geophysics. The wide variety of scientific interests involved has frequently caused an investigator to study the effect of one variable with complete disregard for the constancy of another condition which an investigator in another field had shown to be important.

In 1856, D'Arcy [4] reported the proportionality between pressure drop per unit length of a porous bed and the flow of water through it. In 1863, Dupuit [5] suggested that the apparent liquid velocity based on the cross section of the empty tube must be less than the actual velocity in the pores. If the pore space in the bed is considered to be evenly distributed, the porosity of a layer of infinitesimal thickness normal to the direction of flow will be equal to the porosity, δ, of the bed. Dupuit, therefore, revised the D'Arcy equation to read

$$u=\delta K\Delta P/L.$$

Subsequent investigators ignored this porosity concept for a number of years.

Von Emersleben [6] derived the D'Arcy equation from fundamental hydrodynamic principles.

Arnould's [7] data on air flow through beds of rings, spirals, and triangles led to the following correlation:

$$q=0.0286\sqrt{\Delta P/\rho},$$

where q=air flow, m.^{3}/sec.
ΔP=pressure drop, mm. of H_2O
ρ=air density, kg./m.^{3}

Muskat and Botset [8] obtained data on the flow of air through glass beads, sands, and sandstones which they correlated as

$$\Delta P=K(\rho u)^{3/4}.$$

Schoenborn and Dougherty [9] added to the literature by presenting in graphical form their data on the flow of air, water, and oil through beds of various commercial ring and saddle packings.

White [10] recognized that the inconsistent exponents in the relation between ΔP and u or G, expressed in the above references, were due to the fact that the exponent varied with Reynolds number, much as it does for flow through empty pipes. He attempted to correlate data of other investigators for ring- and saddle-packed beds by plotting f vs. Re, where f is defined by the equation

$$\frac{\Delta P}{L}=\frac{2f\rho u^2F_a}{gD_p}.$$

F_a is an empirical correction factor dependent on particle size. The curves indicated fairly good correlation for individual packings, but the values of f for saddles were two to three times the values for rings at the same Reynolds numbers.

Fancher and Lewis [11] also evaluated f. Their data for flow of air, water, and crude petroleum through beds of sands, sandstones, and lead shot were principally in the viscous range, as shown by the linearity of their log-log curves for:

$$f=\frac{\Delta PD_pg_c}{2\rho Lu^2}=\frac{C}{Re}.$$

C varied with the nature of the packing. The value of D_p, used by Fancher and Lewis, was a weight-mean diameter

$$D_p=[\Sigma w_i(D_i)^3]^{1/3}.$$

Allen [12] obtained similar relationships for the flow of air, naphtha, and mineral oil through

[4] D'Arcy, H. P. G., Les Fontaines Publique de la Ville de Dijon: Paris, 1856.
[5] Dupuit, A. J., Études Theoretiques et Practiques sur le Mouvement des Eaux: Paris, 1863.
[6] von Emersleben, Otto, Das Darcysche Filtergesetz: Physikal. Zeitschrift, vol. 26, 1925, pp. 601–610.
[7] Arnould, J., Corps de Remplissage et de Garnissage et Perte de Charge Creers par Leur Empilages: Jour. Chimie Ind., vol. 21, 1929, pp. 478–482.
[8] Muskat, M., and Botset, H. G., Flow of Gas Through Porous Media: Physics, vol. 1, 1931, pp. 27–34.
[9] Schoenborn, E. M., and Dougherty, W. J., Pressure Drop and Flooding Velocity in Packed Towers with Viscous Liquids: Trans. Am. Inst. Chem. Eng., vol. 40, 1944, pp. 51–77.
[10] White, A. M., Pressure Drop and Loading Velocities in Packed Towers: Trans. Am. Inst. Chem. Eng., vol. 31, 1935, pp. 390–408.
[11] Fancher, G. H., and Lewis, J. A., Flow of Simple Fluids Through Porous Materials: Ind. Eng. Chem., vol. 25, 1933, pp. 1139–1147.
[12] Allen, H. V., Pressure Drop for Flow Through Beds of Granular Absorbents: Petrol. Refiner, vol. 23, 1944, pp. 247–252.

beds of granular absorbents (bauxite and fuller's earth), although he used a reciprocal-volume mean diameter:

$$D_p=\left[\frac{1}{\Sigma w_i/(D_i)^3}\right]^{1/3}.$$

The limits of Allen's data were:

$$0.05<Re<500$$

$$7<f<10^4$$

$$0.0008 \text{ ft.}<D_p \text{ (bauxite)}<0.0091 \text{ ft.}$$

$$0.0011 \text{ ft.}<D_p \text{ (fuller's earth)}<0.0096 \text{ ft.}$$

Fujita and Uchida [13] [14] passed gases through beds of broken limestone, lead shot, and Raschig rings and expressed their results in the form of the equation:

$$\frac{\Delta P}{\rho L}=A\left(\frac{u^2}{2gD_p}\right)^l(Re)^m\left(\frac{D_t}{D_p}\right)^n,$$

where l and n are functions of the packing and A and m are functions of both packing and Reynolds number. Their experimental limits and constants are given in table A.

Gamson, Thodos, and Hougen [15] plotted their observed values of f vs. Re for air flow over wet and dry spheres and cylinders, where they defined

$$f=\frac{\Delta P D_p g_c \rho}{2LG^2}$$

$$Re=D_pG/\mu.$$

For cylinders,

$$D_p=\sqrt{d_c h_c+1/2\,d_c^2}.$$

They obtained separate curves for wet and dry packings.

TABLE A.—*Constants of Uchida and Fujita* [13] [14]

Flow	Packing		
	Broken limestone 5 mm. $<D_p<$ 10 mm.	Lead shot 1.8 mm. $<D_p<$ 4.4 mm.	Raschig rings 5 mm. $<D_p<$ 10 mm.
$10<Re<30$	$A=10{,}600$ $m=-0.87$ $l=1.15$ $n=-0.30$	$A=2{,}400$ $m=0.86$ $l=1.05$ $n=0.0$	$A=350$ $m=-0.64$ $l=0.94$ $n=0.0$
$30<Re<100$	$A=10{,}600$ $m=-0.87$ $l=1.15$ $n=-0.30$	$A=520$ $m=-0.47$ $l=1.05$ $n=0.0$	$A=145$ $m=-0.38$ $l=0.94$ $n=0.0$
$100<Re<1{,}000$	$A=3{,}670$ $m=-0.64$ $l=1.15$ $n=-0.30$	$A=520$ $m=-0.47$ $l=1.05$ $n=0.0$	$A=51$ $m=-0.16$ $l=0.94$ $n=0.0$

In 1932, Chalmers, Taliaferro, and Rawlins [16] introduced the porosity concept into their definition of friction factor f:

$$f=\frac{\Delta P D_p g_c \delta^2}{\rho L u^2}.$$

This concept, which had been developed by Dupuit,[17] had also been used by Boussinesq [18] in a theoretical derivation of formulas similar to those of D'Arcy.

In 1934, Chilton and Colburn [19] had correlated their data for gas flow through packed tubes with a so-called "wall-effect factor, A_f", which, however, implicitly compensated to a certain degree for porosity as well as the effect of the D_p/D_t ratio,

$$\frac{\Delta P}{L}=\frac{2fG^2A_f}{g_c D_p \rho}.$$

f is expressed graphically as a function of Re, and A_f is expressed graphically as a function of D_p/D_t.

Bakhmeteff and Feodoroff [20] defined f by the earlier convention

$$f=\frac{2g_c \Delta P D_p}{\rho L u^2}$$

[13] Uchida, S., and Fujita, S., Pressure Drop Through Dry Packed Towers: Soc. Chem. Ind. (Japan), vol. 37, 1934, pp. 724B–728B.
[14] Fujita, S., and Uchida, S., Pressure Drop Through Dry Packed Towers: Soc. Chem. Ind. (Japan), vol. 37, 1934, pp. 791B–794B.
[15] Gamson, B. W., Thodos, G., and Hougen, O. A., Heat, Mass, and Momentum Transfer in the Flow of Gases Through Granular Solids: Trans. Am. Inst. Chem. Eng., vol. 39, 1943, pp. 1–35.
[16] Chalmers, J., Taliaferro, D. B., and Rawlins, E. L., Flow of Air and Gas Through Porous Media: Trans. Am. Inst. Min. and Met. Eng., Petrol. Div., vol. 98, 1932, pp. 375–400.
[17] Work cited in footnote 5, p. 3.
[18] Boussinesq, M. J., On the Theory of the Transmission of Gases Across Porous Media: Compt. Rend., vol. 159, 1914, pp. 390, 519.
[19] Chilton, T. H., and Colburn, A. P., Pressure Drop in Packed Tubes: Ind. Eng. Chem., vol. 23, 1931, pp. 913–931.
[20] Bakhmeteff, B. A., and Feodoroff, N. V., Flow Through Granular Media: Jour. Appl. Mech., vol. 4, 1937, pp. A97–A104.

but correlated the values of f they obtained for gas flow through beds of lead shot by plotting f against Re and δ. For laminar flow, they obtained

$$f=710/Re\,\delta^{4/3}$$

and for turbulent flow

$$f=24.2/(Re)^{0.2}\delta^{4/3}.$$

For viscous flow of gases and liquids through porous carbon, Hatfield [21] found that his friction factors in the flow range $10^{-5}<Re<10^{2}$ could be linearly correlated with the Reynolds number by defining

$$f=\frac{\Delta P D_p g_c \delta^2}{2G\,L\,u}.$$

It can be seen that this definition is identical with that proposed by Chalmers et al.[22]

Meyer and Work [23] related the bed voidage for a given packing to some value δ_n representing the loosest packing possible for the specified material. They defined

$$D_p=\Sigma w_i D_i$$

and reported

$$\frac{\Delta P}{L}=\frac{K\mu(67-\delta)}{g\left(D_p\frac{\delta}{\delta_n}\right)^2},$$

where K=47.5 for crushed rock and 33.3 for lead shot.

Happel [24] correlated f vs. Re, where f was a function of the relative solids volume $(1-\delta)$:

$$f=\frac{\Delta P D_p g_c \rho}{LG^2(1-\delta)^3}.$$

D_p was defined as

$$\frac{1}{\Sigma\frac{w_i}{D_i}}.$$

Happel reported that for the laminar range $f=103/Re$ and for the turbulent range $f=207/(Re)^{0.22}$.

Just as porosity has been handled by various investigators in various ways—including periods of complete neglect—so was the shape of the particle treated as a factor influencing fluid flow.

In 1934, Wadell [25] defined a shape factor for single particles falling freely through fluids as the ratio of the surface of a sphere having the same volume of the particle to the actual surface of the particle. Zeisberg [26] had published pressure-drop data for various commercial types of packing. Chilton [27] converted these data, as well as the data of White,[28] to values of friction factors for the various shapes for use in his previously published [29] equation.

Blake [30] correlated data on glass cylinders, Raschig rings, and crushed pumice by a linear plot on log-log coordinates of

$$\frac{\Delta P\rho\delta^3}{LG^2S}\text{ vs. }\frac{G}{\mu S},$$

where S is the value of surface area of packing per unit volume of packed tube.

Kozeny [31] showed that this value of S represented a function of diameter and shape of the channel. He derived Blake's equation by assuming that the granular bed was equivalent to a group of similar channels whose total internal surface and volume were equal to the particle surface and pore volume; that is, the mean hydraulic radius of the channel was δ/S.

Furnas [32 33] reported on the effect of a large number of variables. However, he expressed his data in the form

$$\frac{\Delta P}{L}=AG^B,$$

where A and B were complex functions of particle size, bed porosity, and the gas properties temperature, viscosity, density, and molecular weight.

From their studies of spherical lead shot of various sizes in various-diameter tubes, Burke and Plummer [34] concluded that pressure drop is a function of a modified Reynolds number $\frac{u\rho}{\mu S}$, which is equivalent to

$$\frac{GA_p}{\mu V_t}\text{ or }\frac{GA_p(1-\delta)}{\mu V_p};\quad \frac{\Delta P}{L}=\frac{K\rho u^2 S}{\delta^3}\left(\frac{\mu S}{\rho u}\right)^{2-n},$$

where n is a function of the Reynolds number.

Carman [35 36] correlated the pressure-drop data of other authors by the following dimensionally homogeneous formula:

[21] Hatfield, M. R., Fluid Flow Through Porous Carbon: Ind. Eng. Chem., vol. 31, 1939, pp. 1419–1424.
[22] See work cited in footnote 16, p. 4.
[23] Meyer, W. G., and Work, L. T., Flow of Fluids Through Beds of Packed Solids: Trans. Am. Inst. Chem. Eng., vol. 33, 1937, pp. 13–33.
[24] Happel, J., Pressure Drop Due to Vapor Flow Through Moving Beds: Ind. Eng. Chem., vol. 41, 1949, pp. 1161–1174.
[25] Wadell, H., The Coefficient of Resistance for Solids of Various Shapes: Jour. Franklin Inst., vol. 217, 1934, pp. 459–470.
[26] Zeisberg, F. C., The Resistance of Absorption Tower Packing to Gas Flow: Trans. Am. Inst. Chem. Eng., vol. 12, pt. II, 1919, pp. 231–237.
[27] Chilton, T. H., The Science of Petroleum: Oxford University Press, London, 1938, pp. 2211–2222.
[28] See work cited in footnote 10, p. 3.
[29] See work cited in footnote 19, p. 4.
[30] Blake, F. C., The Resistance of Packing to Fluid Flow: Trans. Am. Inst. Chem. Eng., vol. 14, 1922, pp. 415–421.
[31] Kozeny, J., Ber. Wien. Akad., vol. 136a, 1927, pp. 271–278.
[32] Furnas, C. C., Grading Aggregates: Ind. Eng. Chem., vol. 23, 1931, pp. 1052–1058.
[33] Furnas, C. C., The Flow of Gases Through Beds of Broken Solids: Bureau of Mines Tech. Paper 307, 1929, 144 pp.
[34] Burke, S. P., and Plummer, W. B., Gas Flow Through Packed Columns: Ind. Eng. Chem., vol. 20, 1928, pp. 1196–1200.
[35] Carman, P. C., The Determination of the Specific Surface of Powders. I and II: Jour. Soc. Chem. Ind. (London), vol. 57, 1938, pp. 225–234; vol. 58, 1939, pp. 1–7.
[36] Carman, P. C., Fluid Flow Through Granular Beds: Trans. Inst. Chem. Eng. (London), vol. 15, 1937, pp. 150–166.

$$f=\frac{\Delta P g_c \delta^3}{L\rho u^2 S_1}=C\left(\frac{\mu S}{\rho u}\right)^{0.1},$$

where $S_1=S+4/D_t$, C=a constant dependent on particle shape.

For solid spheres and saddles, $C=0.4$.

For ring packings, $C=1.0$.

Hatch [37] developed a dimensionally homogeneous equation for pressure drop in packed tubes which also applies to expanded beds of sands (200-mesh to 20-mesh) under counter-gravity flow of water.

$$\frac{h}{l}=\frac{k}{g_c}\left(\frac{\mu}{\rho}\right)^{2-n} \qquad u^n\left(\frac{A_p}{V_p}\right)^{3-n} \qquad \frac{(1-\delta)^{3-n}}{\delta^3}$$

where

$\frac{h}{l}$=resistance/length of bed (no dimension)

k=a coefficient

n=state of flow factor.

For laminar flow, $n=1$. For turbulent flow, $n=2$.

Oman and Watson [38] correlated their pressure-drop data in the turbulent flow range of air flow through (dense and loose-packed) beds of 0.267-inch celite cylinders, 0.385-inch clay Raschig rings, 0.5-inch clay Berl saddles, 0.2166-inch celite spheres, and 0.1875-inch MgO granules, in a 4-inch standard pipe, with the following equation:

$$\Delta P=\frac{2fLG^2S}{g_c\rho\delta^{1.7}}.$$

Their data covered a flow region of $20<Re<1{,}200$, where Re is defined as

$$\frac{G}{S\mu}.$$

Brownell and Katz [39] correlated pressure-drop data of other investigators with their own data on air flow through 65- to 80-mesh salt beds by means of the following dimensionally homogeneous equation:

$$\Delta P=\frac{fLu^2\rho}{2g_cD_p\delta^n}.$$

The factor "f" may be obtained from the curves of Moody [40] for flow through empty pipes when the Reynolds number is defined as

$$Re=\frac{D_pG}{\mu\delta^m}.$$

The exponents, n and m, are dependent on particle shape and bed porosity and are presented as experimentally derived curves.

Other references pertinent to the subject of fluid flow through packed beds may be found in the work of other investigators.[41-79]

[37] Hatch, L. P., Flow of Fluids Through Granular Materials: Trans. Am. Geophys. Union, vol. 24, 1943, pp. 537-547.
[38] Oman, O. A., and Watson, K. M., Pressure Drop in Granular Beds: Nat. Petrol. News, vol. 36, 1944, pp. R795-802.
[39] Brownell, L. E., and Katz, D. L., Flow of Fluids Through Porous Media. I: Chem. Eng. Prog., vol. 43, 1947, pp. 537-548.
[40] Moody, L. F., Friction Factors for Pipe Flow: Trans. Am. Soc. Mech. Eng., vol. 66, 1944, pp. 671-682.

[41] Bain, W. A., and Hougen, O. A., Flooding Velocities in Packed Columns: Trans. Am. Inst. Chem. Eng., vol. 40, 1944, pp. 29-49.
[42] Bartell, F. E., The Permeability of Porcelain and Copper Ferrocyanide Membranes: Jour. Phys. Chem., vol. 15, 1911, pp. 659-674.
[43] Bartell, F. E., Pore Diameters of Osmotic Membranes: Jour. Phys. Chem., vol. 16, 1912, pp. 318-335.
[44] Bartell, F. E., and Osterhof, H. J., The Pore Size of Compressed Carbon and Silica Membranes: Jour. Phys. Chem., vol. 32, 1938, pp. 1553-1558.
[45] Berg, C., Fawcett, P. N., and Dhondt, R. O., Channeling Effects in Reactors of a Commercial Hydroformer: Chem. Eng. Prog., vol. 43, 1947, pp. 713-730.
[46] Capell, G., Amero, R. C., and Moore, J. W., New Data on Activated Bauxite Desiccants: Chem. Met. Eng., vol. 50, July 1943, pp. 107-110.
[47] Donat, J., The Porosity of Sand: Wasserkraft u. Wasserviteh, vol. 24, 1929, pp. 225-229.
[48] Egolf, C. B., and McCabe, W. L., Rate of Sedimentation of Flocculated Particles: Trans. Am. Inst. Chem. Eng., vol. 33, 1937, pp. 620-642.
[49] Fair, G. M., and Hatch, L. P., The Streamline Flow of Water Through Sand: Jour. Am. Water Works Assoc., vol. 25, 1933, pp. 1551-1557.
[50] Fehling, R., Der Strömungswiderstand Ruhender Schüttungen: Feuerungstechnik, vol. 27, 1939, pp. 33-40.
[51] Graton, L. C., and Fraser, H. J., Systematic Packing of Spheres: Jour. Geol., vol. 43, 1935, pp. 785-909.
[52] Givan, C. V., Flow of Water Through Granular Materials: Trans. Am. Geophys. Union, vol. 15, 1934, p. 572.
[53] Hancock, R. T., Interstitial Flow: Min. Mag., vol. 67, 1942, pp. 179-186.
[54] Heywood, H., Numerical Definitions of Particle Size and Shape: Jour. Soc. Chem. Ind., vol. 56, 1937, pp. 149-154.
[55] Hickox, G. A., Flow Through Granular Materials: Trans. Am. Geophys. Union, Part 2, 1934, pp. 567-572.
[56] Hirst, A. A., Separation of Particles by Virtue of Density Difference: Trans. Inst. Min. Eng. (London), vol. 85, 1932-33, pp. 236-241.
[57] Hirst, A. A., Theories of Gravity Separation: Trans. Inst. Min. Eng. (London), vol. 94, 1937-38, pp. 93-113.
[58] Kermack, W. A., M'Kendrick, A. G., and Ponder, E., The Stability of Suspensions: Proc. Roy. Soc. (Edinburgh), vol. 49, 1929, pp. 170-197.
[59] Lapple, C. E., and Shepherd, C. B., Calculation of Particle Trajectories: Ind. Eng. Chem., vol. 32, 1940, pp. 605-617.
[60] Lapple, C. E., Mist and Dust Collection in Industry and Buildings: Heating, Piping, Air Conditioning, vol. 17, 1945, pp. 611-615.
[61] Mach, E., Druckverluste und Belastungs Grenzen von Fuelkörpersäulen Forschungsheft vol. 375, 1935, V. D. I.; Apparatebau, vol. 50, 1938, pp. 124-7, 135-7.
[62] Mavis, F. T., and Wilsey, E. F., A Study of the Permeability of Sand: Univ. of Iowa Study Bull. 7, 1937.
[63] Meldou, R., and Stach, E., The Fine Structures of Powders in Bulk with Special Reference to Pulverized Coal: Trans. Jour. Inst. Fuel, vol. 7, 1934, pp. 336-354.
[64] Newton, R. H., Dunham, G. S., and Simpson, T. P., The T. C. C. Process for Motor Gasoline Production: Trans. Am. Inst. Chem. Eng., vol. 41, 1945, pp. 215-232.
[65] Rose, H. E., The Laws of the Flow of Fluids Through Beds of Granular Materials: Proc. Inst. Mech. Eng., vol. 153, 1945, pp. 141, 148, and 154.
[66] Saunders, D. A., and Ford, H., Heat Transfer in the Flow of Gas Through a Bed of Solid Particles: Jour. Iron and Steel Inst., vol. 141, 1940, pp. 138-144.
[67] Sherwood, T. K., Pressure Drop Through Packings. *In* Absorption and Extraction: McGraw Hill Publishing Co., Inc., New York, 1937, pp. 138-144.
[68] Schriever, W., Passage of a Gas-Free Liquid Through Spherical-Grained Sand: Trans. Am. Inst. Min. and Met. Eng., vol. 86, 1930, pp. 329-336.
[69] Slichter, C. S., Rectilinear Flow of Ground Water Through a Soil: U. S. Geol. Survey, 19th Ann. Report, vol. 2, 1897-8, pp. 305-311.
[70] Smith, W. O., Capillary Flow Through an Ideal Uniform Soil: Physics, vol. 1, 1931, pp. 18-24.
[71] Smith, W. O., Busang, P. F., and Foote, P. D., Capillary Rise in Sands of Uniform Spherical Grains: Physics, vol. 1, 1931, pp. 18-24.
[72] Steinour, H. H., Rate of Sedimentation. I, II, and III: Ind. Eng. Chem., vol. 36, 1944, pp. 618, 840, and 901.
[73] Sullivan, R. R., and Hertel, K. L., The Flow of Air Through Porous Media: Jour. Applied Physics, vol. 11, 1940, pp. 761-765.
[74] Terzaghi, C., Determination of the Permeability of Clay: Chem. Eng. News, vol. 95, 1925, pp. 832-836.
[75] Traxler, R. N., and Baum, L. A. H., Permeability of Compacted Powders—Pore Size: Physics, vol. 7, 1936, pp. 9-14.
[76] Trumpler, P. R., and Dodge, B. F., Design of Ribbon-Packed Exchangers: Chem. Eng. Prog., vol. 43, 1947, pp. 75-84.
[77] Weedman, J. A., and Dodge, B. F., Rectification of Liquid Air in a Packed Column: Ind. Eng. Chem., vol. 39, 1947, pp. 732-744.
[78] Work, L. T., and Kohler, A. S., The Sedimentation of Suspensions: Trans. Am. Inst. Chem. Eng., vol. 36, 1940, pp. 701-719.
[79] Zakharov, B. A., and Frost, A. V., Pressure Drop Through Granular Materials in Contact Packed Tubes: Bull. Acad. Sci., U. S. S. R., Classe, Sci. Tech., 1946, pp. 421-441.

FLUIDIZATION

Despite a number of years of commercial application of fluidization techniques, no quantitative data appeared in the literature prior to 1947.

A number of articles have appeared in which various qualitative aspects of fluidization are discussed, particularly as applicable to catalytic cracking [80–83] and other functions in the petroleum industry.[84–86]

Kite and Roberts[87] discuss the application of fluidization to the process of calcination of limestone.

A number of articles have appeared on processes similar to fluidization, such as the backwashing of water filtration sand beds[88] and solids elutriation with liquids or gases.[89–93]

Parent, Yagol, and Steiner[94] discussed a number of qualitative aspects of fluidization design and reported that the pressure drop across a fluidized bed was approximately equal to the weight of the solids per unit cross section of the bed.

Wilhelm and Kwauk[95] presented some fundamental data that were subsequently discussed by Morse.[96] The two papers are treated in more detail in a subsequent section.[97]

In 1948 and 1949, a number of papers appeared on various restricted but important topics.

Logwinuk[98] carried out an extensive study of fluid and heat flow in which air, carbon dioxide, and helium were used to fluidize a variety of solids. The basic similarity between flow through fixed and fluidized beds was stressed by Ergun and Orning,[99] and a 2-term data correlation was proposed. Lewis et al.[1] investigated both batch and continuous fluidization of glass spheres of various sizes. The Stormer viscosity of aerated beds was measured and analyzed by Matheson[2] et al., and Beck[3] reported on the use of stirrers and baffles as aids to fluidization.

By means of temperature measurements and a tracer gas, Gilliland and Mason[4] studied the mixing and back mixing of both the solids and gases in small-diameter fluidized beds. Meissner and Mickley[5] revealed that fluidized beds possess a definite capacity for filtering fine mists and dusts.

A number of additional papers[6–13] have appeared describing the application of fluidization to more processes, and a few other recent papers[14–17] have added to the literature on the associated subjects of attrition, erosion, and solids flow.

---

[80] Thomas, C. L., Anderson, N. K., Becker, H. A., and McAfee, J., Cracking with Catalysts: Proc. Am. Petrol. Inst., vol. 24, sec. 3, 1943, pp. 75–82.
[81] Wickham, H. P., Mechanism of Flow in Fluid-Catalyst Cracking: Petrol. Refiner, vol. 24, July 1945, pp. 233–236.
[82] Carlsmith, L. E., and Johnson, F. B., Pilot-Plant Development of Fluid Catalytic Cracking: Ind. Eng. Chem., vol. 37, 1945, pp. 451–455.
[83] Murphree, E. V., et al., Improved Fluid Process for Catalytic Cracking: Trans. Am. Inst. Chem. Eng., vol. 41, 1945, pp. 19–33.
[84] Thomas, C. L., and Hoekstra, J., Fluidized Fixed Bed: Ind. Eng. Chem., vol. 37, 1945, pp. 332–334.
[85] Murphree, E. V., Gohr, E. J., and Kaulakis, A. F., The Fluids-Solids Technique—Applications in the Petroleum Industry: Jour. Inst. Petrol., vol. 33, 1947, pp. 608–620.
[86] Egloff, G., Le Cracking Catalytique: Chimie et Industrie, vol. 59, 1948, pp. 121–127.
[87] Kite, R. P., and Roberts, E. J.: Chem. Eng., vol. 54, No. 12, Dec. 1947, pp. 112–115.
[88] Hatch, L. P., Flow Through Granular Media: Trans. Am. Soc. Mech. Eng., vol. 62, 1940, pp. A103–A112.
[89] Martin, G., Researches on the Theory of Fine Grinding: Trans. Ceramic Soc., vol. 25, 1926–7, pp. 21–33.
[90] Crump, W., Pneumatic Transport of Plants: Chem. Ind. (London), vol. 44, 1925, pp. 207T–213T.
[91] Burke, S. P., and Plummer, W. B., Suspension of Macroscopic Particles in a Turbulent Gas Stream: Ind. Eng. Chem., vol. 20, 1928, pp. 1200–1204.
[92] Wadell, H., Sedimentation Formulas: Physics, vol. 5, 1934, pp. 281–241.
[93] Camp, T. R., Sedimentation and Design of Settling Tanks: Proc. Am. Soc. Civil Eng., vol. 71, 1945, pp. 445–486.
[94] Parent, J. D., Yagol, N., and Steiner, C. S., Fluidizing Process: Chem. Eng. Progress, vol. 43, 1947, pp. 429–436.
[95] Wilhelm, R. H., and Kwauk, M., The Fluidization of Solid Particles: Chem. Eng. Prog., vol. 44, 1948, pp. 201–218.
[96] Morse, R. D., Fluidization of Granular Solids: Ind. Eng. Chem., vol. 41, 1949, pp. 1117–1124.
[97] See discussion, p. 82.

[98] Logwinuk, A. K., Ph. D. Thesis: Case Institute of Technology, August 1948.
[99] Ergun, S., and Orning, A. A., Fluid Flow Through Randomly Packed Columns and Fluidized Beds: Ind. Eng. Chem., vol. 41, 1949, pp. 1179–1184.
[1] Lewis, W. K., Gilliland, E. R., and Bauer, W. C., Characteristics of Fluidized Particles: Ind. Eng. Chem., vol. 41, 1949, pp. 1104–1117.
[2] Matheson, G. L., Herbst, W. A., and Holt, P. H., Characteristics of Fluid-Solid Systems: Ind. Eng. Chem., vol. 41, 1949, pp. 1099–1104.
[3] Beck, R. A., Evaluation of Fluid Catalyst. Laboratory Scale: Ind. Eng. Chem., vol. 41, 1949, pp. 1242–1243.
[4] Gilliland, E. R., and Mason, E. A., Gas and Solid Mixing in Fluidized Beds: Ind. Eng. Chem., vol. 41, 1949, pp. 1191–1196.
[5] Meissner, H. P., and Mickley, H. S., Removal of Mists and Dusts from Air by Beds of Fluidized Solids: Ind. Eng. Chem., vol. 41, 1949, pp. 1238–1242.
[6] Nicholson, E. W., Moise, J. E., and Hardy, R. L., Fluidized-Solids Pilot Plants: Ind. Eng. Chem., vol. 40, 1948, pp. 2033–2039.
[7] Lewis, W. K., Gilliland, E. R., and Reed, W. A., Reaction of Methane with Copper Oxide in a Fluidized Bed: Ind. Eng. Chem., vol. 41, 1949, pp. 1227–1237.
[8] Lewis, W. K., Gilliland, E. R., and McBride, G. T., Jr., Gasification of Carbon by Carbon Dioxide in a Fluidized Bed: Ind. Eng. Chem., vol. 41, 1949, pp. 1213–1226.
[9] Singh, A. D., and Kane, L. J., Fluid Devolatilization of Coal for Power-Plant Practice: Trans. Am. Soc. Mech. Eng., vol. 70, 1948, pp. 957–964.
[10] Parry, V. F., Goodman, J. B., and Wagner, E. O., Drying Low-Rank Coals in the Entrained and Fluidized State: Mining Eng., vol. 1, sec. 3, April 1949, pp. 95–98.
[11] Dimitri, M. S., Jongedyk, R. P., and Lewis, H. C., Distillation of Fluidized Hard Wood: Chem. Eng., vol. 55, No. 12, 1948, pp. 124–125.
[12] Wall, C. J., and Ash, W. J., Fluid-Solid Air Sizer and Dryer: Ind. Eng. Chem., vol. 41, 1949, pp. 1247–1249.
[13] Canadian Chemical Process Industries, Oil Recovery by Fluidization: Vol. 33, No. 2, February 1949, p. 123.
[14] Stoker, R. L., Erosion Due to Dust Particles in a Gas Stream: Ind. Eng. Chem., vol. 41, 1949, pp. 1196–1199.
[15] Forsythe, W. L., Jr., and Hertwig, W. R., Attrition of Fluid Cracking Catalysts: Ind. Eng. Chem., vol. 41, 1949, pp. 1200–1206.
[16] Albright, C. W., Holden, J. H., Simons, H. P., and Schmidt, D. L., Pneumatic Feeder for Finely Divided Solids: Chem. Eng., vol. 56, No. 6, 1949, pp. 108–111.
[17] Schnacky, J. F., New Way to Pressure-Seal Solids Flowing Through a Continuous Process: Chem. Eng., vol. 55, No. 8, 1948, pp. 124–126.

PRESSURE DROP THROUGH PACKED TUBES, TURBULENT FLOW

GENERAL CORRELATION

VARIABLES

Orienting experimental runs and a survey of the literature indicated that the nature of the pressure drop obtained in a packed tube is rather complex. The variables upon which the pressure drop depends may be considered under two general classifications, as follows:

A. Variables related to the fluid flowing through the bed:
   1. Weight rate of flow.
   2. Density of fluid.
   3. Viscosity of fluid.

B. Variables related to the nature of the bed:
   1. Diameter of tube.
   2. Diameter of packing.
   3. Fraction of effective voids.
   4. Shape of particle.
   5. Surface roughness of particle.
   6. Orientation of particles.

This study is concerned with the effect of all of the above variables with the exception of the orientation of the particles. Because, in most industrial applications, the beds are prepared simply by dumping the packing material into the tubes, little or no control can be exercised over arrangement of the particles; however, it is believed that the configurations that arise from dumping are not sufficiently different from each other to affect results significantly.

The general plan followed in order to arrive at a workable correlation was:

a. Derivation of a working equation.
b. Procurement of experimental data with smooth particles.
c. Correlation of data.
d. Comparison of correlation with the working equation.
e. Investigation of the effect of particle roughness upon pressure drop.

DERIVATION OF A WORKING EQUATION

To arrive at a suitable equation describing flow through packed columns, it may be convenient to begin with the general flow equations pertaining to empty pipes:

$$\Delta p=\frac{\Delta P}{L}=\frac{\rho u^2}{g_c D_t}\,\phi\left(\frac{D_t u\rho}{\mu}\right)^{n-2}=\frac{\rho u^2}{g_c D_t}\,k\left(\frac{D_t u\rho}{\mu}\right)^{n-2};$$

$$\Delta p=\frac{k}{g_c}\,\frac{\mu^{2-n}}{\rho^{1-n}}\,u^n D_t^{n-3}. \qquad (1)$$

Earlier experimental orienting observations made in connection with pressure drop through packed columns and fluidization of solid particles suggested that equation (1) be modified according to the assumption of Fair and Hatch,[18] Thus, the velocity through the voids can be expressed by

$$\frac{u}{k_\delta \delta}, \qquad (2)$$

where u is the average velocity of the fluid approaching the bed; k_δ, the proportion of voids in the bed that are effective as far as fluid flow through them is concerned; and δ, the porosity ratio expressed as void volume per unit of packed tube volume.

Furthermore, assuming that the dimensions of the voids are of the same order of magnitude as the particle diameter, then $D_p=4r$, where r is a modified hydraulic radius of the interstices. By definition, let

$$r=\frac{\text{effective volume of the packing interstices}}{\left(\begin{matrix}\text{effective surface}\\ \text{of particles}\end{matrix}\right)\left(\begin{matrix}\text{particle shape}\\ \text{factor}\end{matrix}\right)},$$

or

$$r=\frac{k_\delta V_p \delta}{(1-\delta)k_a \lambda A}, \qquad (3)$$

where A is the surface; V_p, the volume of one packing particle; k_a, the proportion of the effective area of the packing; and λ, an area-volume shape factor to be defined later.

By substituting (2) and (3) into (1), one obtains

$$\Delta p=\frac{k}{g_c}\left(\frac{\mu^{2-n}}{\rho^{1-n}}\right)\left(\frac{u}{k_\delta\delta}\right)^n\left(\frac{k_\delta}{k_a}\,\frac{\delta}{1-\delta}\,\frac{V_p}{A\lambda}\right)^{n-3}. \qquad (4)$$

Substituting

$$\frac{6}{D_p}$$

(the expression for spheres) for

$$\frac{A}{V_p}$$

and G for ρu and rearranging, equation (4) becomes:

$$\Delta p=\frac{k}{g_c}\left(\frac{D_p G}{\mu}\right)^n\left(\frac{\mu^2}{\rho}\right)\left(\frac{\lambda^{3-n}}{D_p^3}\right)\frac{(1-\delta)^{3-n}}{\delta^3}. \qquad (5)$$

[18] Work cited in footnote 49, p. 6.

Empirically, it was found from experiments with empty tubes that exponent n can have any value between 1 and 2, depending on the state of flow. For completely laminar motion, $n=1$, whereas, for completely turbulent conditions, $n \longrightarrow 2$.

SHAPE FACTOR

In order to define the shape factor, λ, in equation (5) let

D_m=average diameter of a particle of any arbitrary shape;
D_p=diameter of a sphere of equivalent volume;
A=surface area of a particle of arbitrary shape; and
A_p=surface area of a sphere of equivalent volume.

Then, $A=\alpha D_m^2$, where α is an area shape factor, and $A_p=\pi D_p^2$.

$$\therefore, \alpha_p=\pi$$

for the sphere of equivalent volume.

By earlier definition, V was designated as the volume of the particle. Then,

$$V_p=\gamma D_m^3=\frac{1}{6} D_p^3,$$

where γ is a volume shape factor.

$$\therefore, \gamma_p=\frac{\pi}{6}$$

for the sphere of equivalent volume.
By definition let

$$\lambda=\frac{A}{A_p}=\frac{\alpha D_m^2}{\pi D_p^2}. \tag{6}$$

Since

$$V_p=\gamma D_m^3=\frac{\pi}{6} D_p^3,$$

solution for D_p yields:

$$D_p=1.241\,\gamma^{1/3} D_m. \tag{7}$$

Substituting (7) into (6) yields

$$\lambda=\frac{0.642\,\alpha D_m^2}{\pi\gamma^{2/3} D_m^2}=0.205\,\frac{\alpha}{\gamma^{2/3}}. \tag{8}$$

For any particle,

$$\frac{A}{V_p}=\frac{\alpha}{\gamma}\,\frac{1}{D_m};$$

substituting this into (8) and recalling that $D_m \gamma^{1/3}=V_p^{1/3}$, yields

$$\lambda=0.205\,\frac{A}{V_p^{2/3}}. \tag{9}$$

EXPERIMENTAL WORK

In order to evaluate k and n in equation (5), experimental data are needed. Preliminary experiments revealed the extraordinary effect that the voids in the bed and the degree of surface roughness of the packing exert upon the pressure drop. Because literature data only infrequently account for the void effect, and because surface roughness had so far not been considered, the work of other investigators could not be used in this correlation; for this reason, an entirely new set of experimental data was obtained in an effort to support equation (5). The experimental work is reported in table I of the appendix of this paper, and a description of the experimental unit is given in figure 1. Wherever necessary, corrections were made for the pressure drop across the screen and the first layer of packing material on top of the screen.

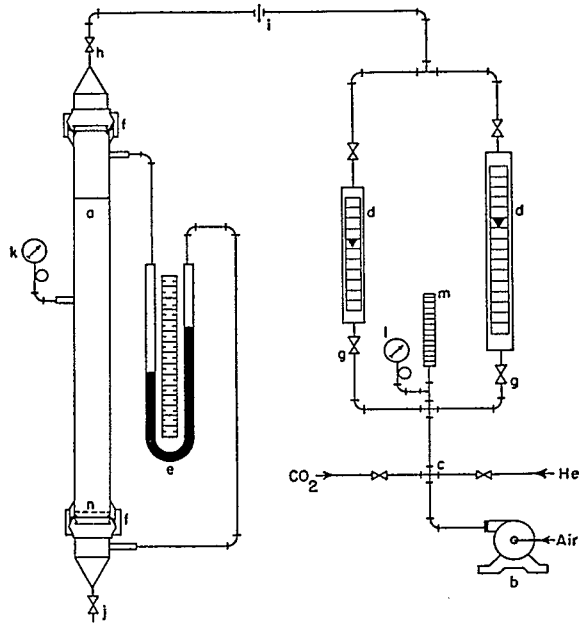

a–Pressure drop tube (1–3 inches dia. interchangeable unions)
b–Air blower.
c–Gas manifold (cross)
d–Rotameters.
e–Manometer.
f–Charge and discharge unions.
g–Control (silencing) valve.
h–Secondary control (silencing) valve.
i–Union.
j–Primary control valve.
k–Pressure gage for total pressure.
l–Rotameter pressure gage.
m–Rotameter thermometer.
n–Supporting screen.

FIGURE 1.—DIAGRAM OF APPARATUS FOR PRESSURE-DROP STUDIES.

Systematic experiments were performed using 0.75-inch, 1-inch, 2-inch, and 3-inch standard pipes. Using logarithmic coordinates, a preliminary plot of pressure drop versus mass velocity was made. The average slope (n) of the lines was 1.90. Because from equation (5) it appears that Δp is proportional to

$$\frac{(1-\delta)^{3-n}}{\delta^3},$$

substitution of $n=1.90$ yields:

$$\Delta p \propto \frac{(1-\delta)^{1.10}}{\delta^3}.$$

Since for practical purposes $(1-\delta)^{1.1}$ is approximately equal to $(1-\delta)$, one may write:

$$\Delta p \propto \frac{(1-\delta)}{\delta^{3.0}}. \qquad (10)$$

Table 1, the key to figures 2 to 6, indicates the wide range of test conditions. In the

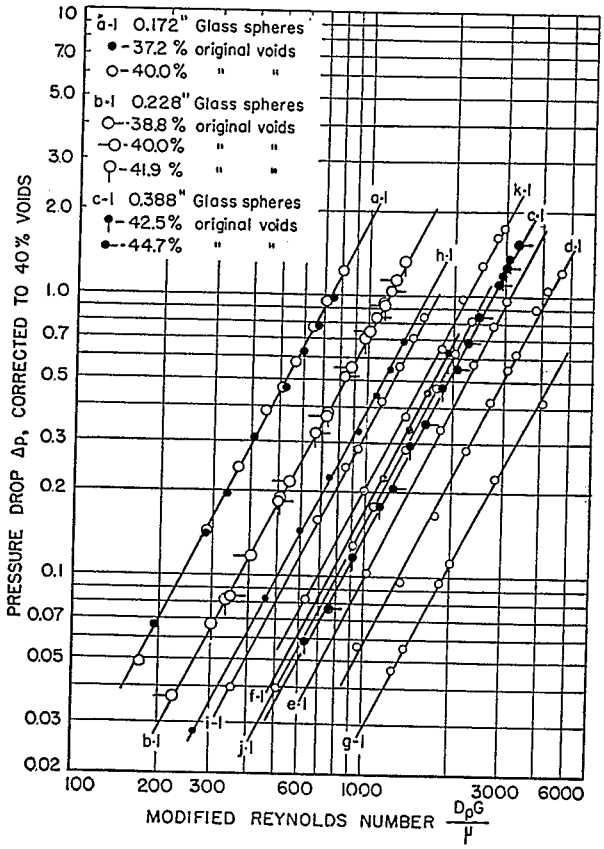

FIGURE 2.—PRESSURE DROP CORRECTED TO 40 PERCENT VOIDS VS. MODIFIED REYNOLDS NUMBER (2-INCH STANDARD PACKED TUBE).

graphs, pressure drops refer to 1 foot of packed height and were corrected to 40 percent voids by using relation (10). The choice of 40 percent as a reference state was arbitrary, and any other value except near 0 and 100 percent could have been chosen. Using logarithmic coordinates, Δp_{40} was plotted against the respective modified Reynolds number, $\frac{D_p G}{\mu}$. The average slope of the lines is 1.90, just as was found earlier for the preliminary plots of Δp versus G. Data pertaining to runs

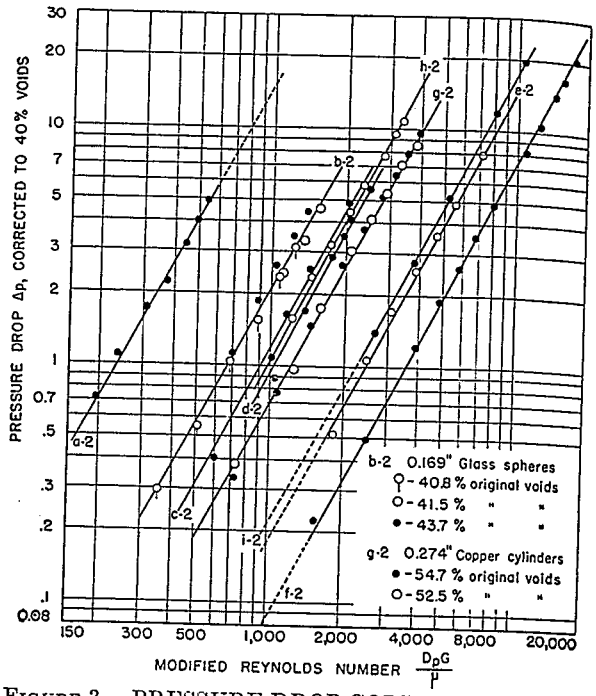

FIGURE 3.—PRESSURE DROP CORRECTED TO 40 PERCENT VOIDS VS. MODIFIED REYNOLDS NUMBER (¾-INCH STANDARD PACKED TUBE).

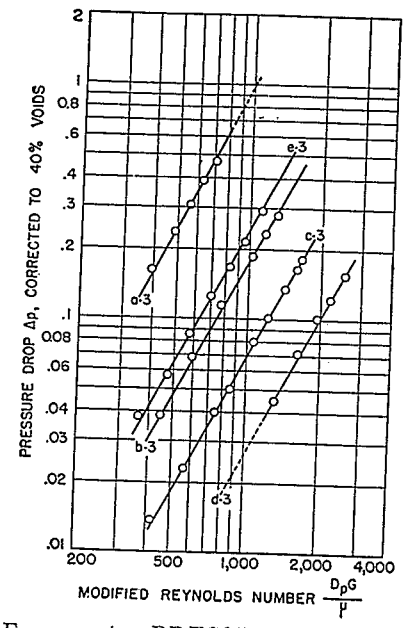

FIGURE 4.—PRESSURE DROP CORRECTED TO 40 PERCENT VOIDS VS. MODIFIED REYNOLDS NUMBER (3-INCH STANDARD PACKED TUBE).

TABLE 1.—*Key to figures 2 to 6*

Run No.	D_p, inches	D_t, inches	$\frac{D_p}{D_t}$	Δp_{40} at Re 1,000	ρ	Shape	Nominal dimensions, inches	Shape factor	Remarks [1]
a-1	0.172	2.067	0.083	1.860	0.0886	Spheres	See D_p	1	
b-1	.228	2.067	.110	.720	.0884	do	do	1	
c-1	.388	2.067	.188	.139	.0871	do	do	1	
d-1	.5075	2.067	.245	.058	.0860	do	do	1	
e-1	.5075	2.067	.245	.100	.0680	do	do	1	Air at 223° F.
f-1	.5075	2.067	.245	.168	.0527	do	do	1	Air at 340° F.
g-1	.5075	2.067	.245	.285	.1175	do	do	1	CO_2 at 82° F.
h-1	.297	2.067	.144	.390	.0882	do	do	1	Nonuniform packing.[7]
i-1	.314	2.067	.152	.330	.0875	do	do	1	do
j-1	.393	2.067	.190	.156	.0879	do	do	1	do
k-1	.403	2.067	.204	.210	.0864	Cylinders [2]	5/16 x 3/8 in. D	1.160	Pellet $\frac{h}{d_c}$=0.833.
a-2	.0885	.824	.107	15.00	.0840	Spheres	See D_p	1	
b-2	.169	.824	.205	2.10	.0840	do	do	1	
c-2	.204	.824	.248	1.20	.0833	do	do	1	
d-2	.224	.824	.272	.94	.0843	do	do	1	
e-2	.391	.824	.474	.18	.0826	do	do	1	
f-2	.5075	.824	.615	.085	.0810	do	do	1	
g-2	.274	.824	.332	.700	.0830	Cylinders [3]	0.247 x 0.236 in. D	1.145	Pellet $\frac{h}{d_c}$=1.048.
h-2	.254	.824	.308	1.040	.0825	do [4]	0.232 x 0.217 in. D	1.147	Pellet $\frac{h}{d_c}$=1.070.
i-2	.403	.824	.490	.215	.0810	Cylinders [2]	See k-1	See k-1	See k-1.
a-3	.228	3.068	.074	.990	.0762	Spheres	See D_p	1	
b-3	.388	3.068	.127	.179	.0750	do	do	1	
c-3	.5075	3.068	.166	.068	.0751	do	do	1	
d-3	.7300	3.068	.238	.0268	.0745	do	do	1	
e-3	.403	3.068	.132	.0236	.0755	Cylinders [2]	See k-1	See k-1	See k-1.
a-4	.188	1.049	.179	2.480	.0870	do [5]	0.263 x 0.128 in. D	1.220	Pellet $\frac{h}{d_c}$=2.06.
b-4	.350	1.049	.334	.540	.0830	Rings [6]	3/8 x 3/8 x 1/4 in. D	2.180	Pellet $\frac{h}{d_c}$=1.00.
c-4	.420	1.049	.400	.180	.0830	Cylinders [3]	1/2 x 5/16 in. D	1.175	Pellet $\frac{h}{d_c}$=1.60.
d-4	.393	1.049	.375	.130	.0830	Spheres	See D_p	1	
e-4	.5075	1.049	.484	.0725	.0830	do	do	1	
f-4	.403	1.049	.384	.175	.0820	Cylinders [2]	See k-1	See k-1	See k-1.
a-5	.228	1.049	.217	.750	.0785	Spheres	See D_p	1	Nitrogen at 75° F. and various pressures.
b-5	.228	1.049	.217	.590	.1040	do	do	1	
c-5	.228	1.049	.217	.445	.1355	do	do	1	
d-5	.228	1.049	.217	.372	.1670	do	do	1	
e-5	.228	1.049	.217	.345	.1840	do	do	1	

[1] Except when mentioned otherwise, run was made with air of average temperature, 75° F.
[2] Tungsten sulfide, coal-hydrogenation catalyst.
[3] Copper cylinders.
[4] Aluminum cylinders.
[5] Cobalt oxide, Fischer-Tropsch catalyst.
[6] Brass rings.
[7] Diameter of mixed packings calculated according to equation 20, p. 26.

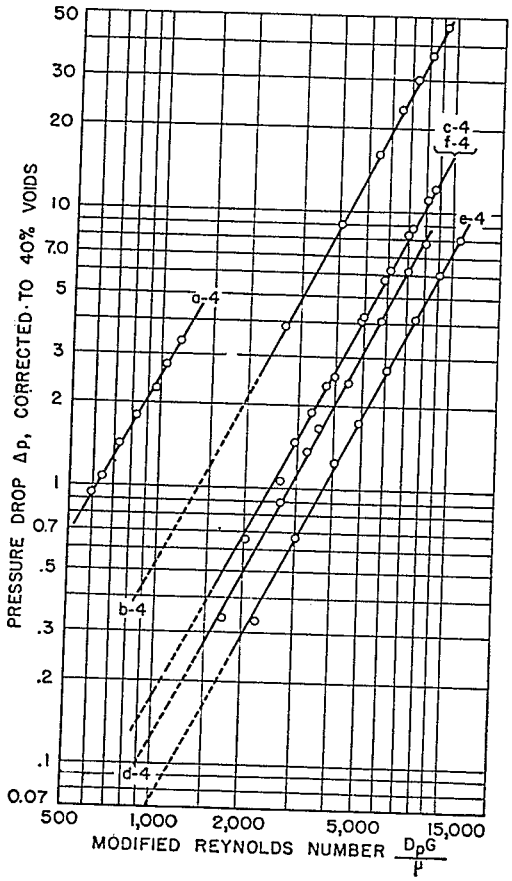

FIGURE 5.—PRESSURE DROP CORRECTED TO 40 PERCENT VOIDS VS. MODIFIED REYNOLDS NUMBER (1-INCH STANDARD PACKED TUBE).

a–1, b–1, c–1, b–2, and g–2 refer to spheres of various diameters and to cylinders, either in a 2-inch or 0.75-inch pipe. For each run, pressure-drop measurements were made to two or three different bed voidages, and it was observed that, for example, a variation of voids from 40 to 43 percent reduced the pressure drop 23 percent. The fact that the data, referred to $\delta=0.40$, fall on one line indicates that relation (10) is generally valid for all particle and tube diameters and shapes.

Figure 6 shows data obtained with nitrogen under five different pressures. During these runs, configuration and other bed properties remained unchanged, and the pressure drop across the tube was small compared with the static fluid pressure. Figure 7 shows the relationship between Δp_{40} and the average gas density plotted on log-log paper. The slope of the straight line is (—1.0), confirming the observation that

$$\Delta p \propto \frac{1}{\rho}.$$

In figure 8, $\rho\Delta p_{40}$ is shown versus the gas viscosity. Logarithmic coordinates were used, and the runs pertain to air and carbon dioxide at different temperatures. Here, too, the bed characteristics remained undisturbed in order to exclude any additional variables. For the range of conditions investigated, the data fall on a straight line, of slope (+2.00), indicating that $\rho\Delta p \propto \mu^2$.

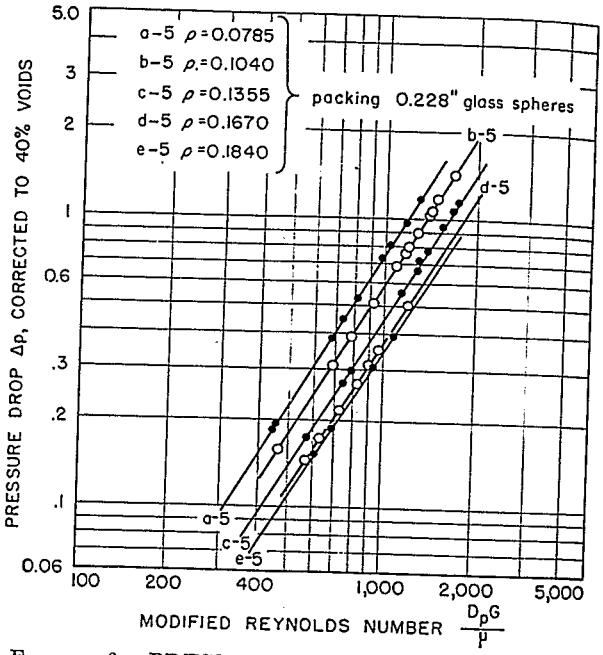

FIGURE 6.—PRESSURE DROP OF NITROGEN AT VARIOUS TOTAL GAS PRESSURES (1-INCH STANDARD PACKED TUBE).

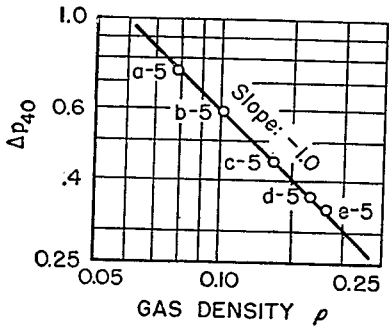

FIGURE 7.—PRESSURE DROP VS. GAS DENSITY (1-INCH STANDARD PACKED TUBE, NITROGEN DATA).

In order to show how Δp varies with D_n, the quantity

$$\frac{\rho\Delta p_{40}}{\lambda^{1.1}},$$

obtained from all the data at Reynolds number 1,000, was plotted in figure 9 against D_p. By

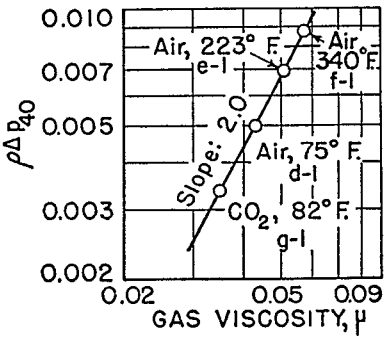

FIGURE 8.—$\rho\Delta p_{40}$ VS. GAS VISCOSITY FOR CO_2 AND AIR (2-INCH STANDARD PACKED TUBE).

using logarithmic coordinates, a straight-line relationship of slope (−3.00) was obtained, indicating that

$$\Delta p \propto \frac{1}{D_p^{3.00}}.$$

A summary of the various results indicates that, according to figures 2 to 6,

$$\Delta p \propto \frac{(1-\delta)}{\delta^3}\left(\frac{D_p G}{\mu}\right)^{1.9};$$

similarly, for figure 7, $\Delta p \propto \frac{1}{\rho}$, figure 8, $\Delta p \propto \mu^2$, and figure 9, $\Delta p \propto \frac{1}{D_p^{3.00}}$.

Combining these proportions results in:

$$\Delta p \propto \frac{(1-\delta)}{\delta^3}\left(\frac{D_p G}{\mu}\right)^{1.9}\frac{\mu^2\lambda^{1.1}}{\rho D_p^{3.00}} = k\frac{G^{1.9}\mu^{0.1}}{D_p^{1.1}}\frac{\lambda^{1.1}(1-\delta)}{g\rho\delta^3}. \quad (11)$$

It will be observed that the experimental equation (11) is identical with equation (5), which was derived earlier. After evaluating k from all the data and averaging, the final equation becomes:

$$\Delta p = \frac{3.50 G^{1.9}\mu^{0.1}\lambda^{1.1}(1-\delta)}{D_p^{1.1}\rho g_c\delta^3}. \quad (12)$$

In figure 10, modified friction factors have been plotted against modified Reynolds numbers. The points fall along a curve, the slope of which varies between (−0.25) for the low Reynolds-number range to zero in the limit

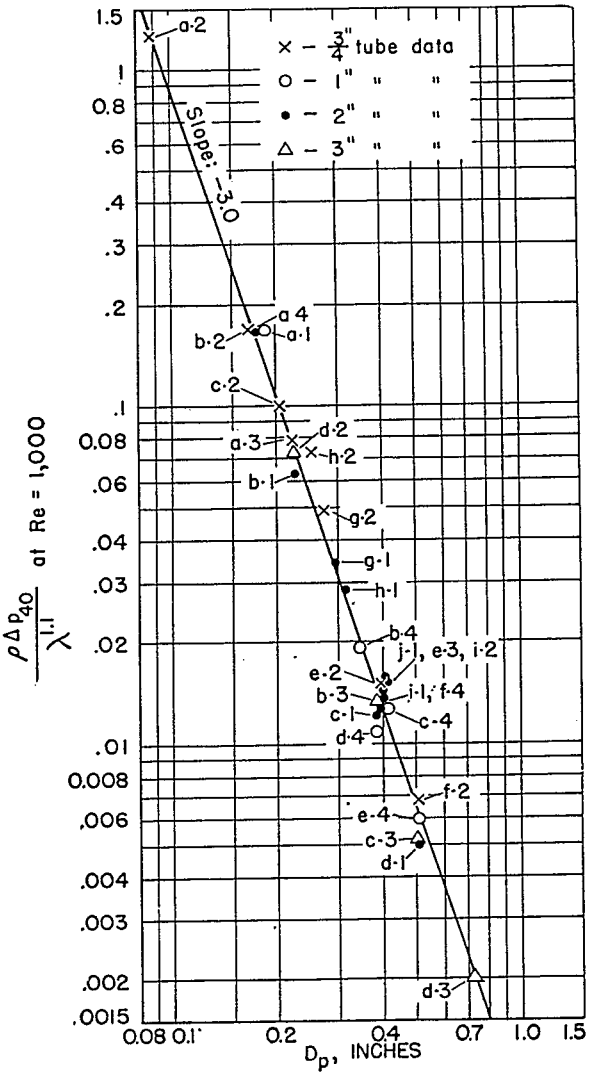

FIGURE 9.—RELATIONSHIP BETWEEN PRESSURE DROP AND PARTICLE DIAMETER.

for the high-turbulence range. The curve may, however, be replaced satisfactorily by a straight line, the equation of which is given by:

$$f = 1.75\left(\frac{D_p G}{\mu}\right)^{-0.1}. \quad (13)$$

In terms of a modified friction factor, f, equation (12) may then be written:

$$\Delta p = \frac{2 f G^2\lambda^{1.1}(1-\delta)}{D_p\rho\delta^3 g_c}. \quad (14)$$

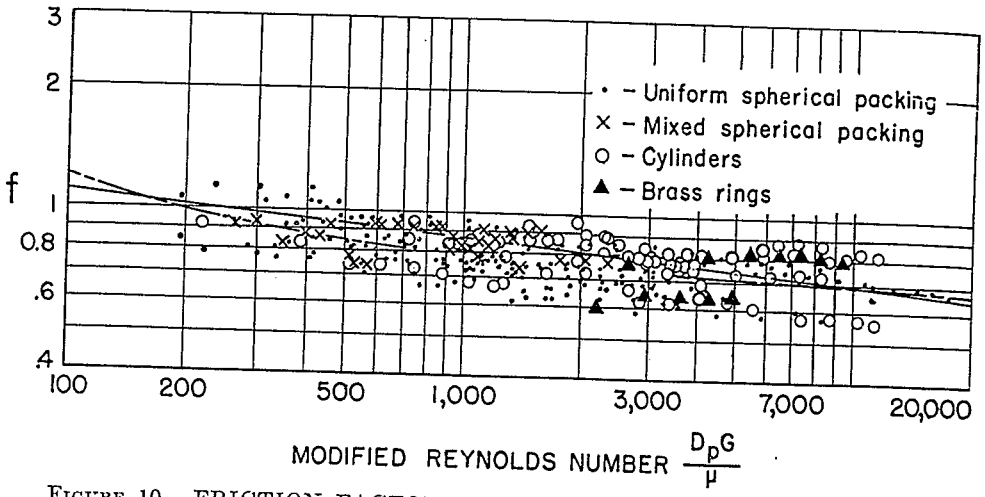

FIGURE 10.—FRICTION FACTOR VS. MODIFIED REYNOLDS NUMBER.

DISCUSSION OF RESULTS

Consideration of equations (13) and (14) reveals that all quantities with the exception of λ and δ are readily available from process specifications. It appears, therefore, that the usefulness of the equations can be greatly increased by developing correlations which permit prediction of λ and δ. Such developments have been attempted and are reported in a later section.

In the derivation of λ, no restrictions were imposed on the shape of the particles of diameter D_m. This would possibly suggest that the factor should apply to a considerable variety of particles, however complex. Fair substantiation of this is found in figure 10, which shows modified friction factors for rings, cylinders, and spheres to be in essential agreement with each other. Later work will demonstrate that data observed with Berl saddles, shapes that are considerably more complex than rings, also fall in line.

For particles of simple geometric shape, the shape factor may readily be calculated from the particle dimensions. For more complex shapes, λ is best found by actual experiment. Usually the total voids, δ, can be determined by immersion. If the particles are porous, the crevices may be filled with paraffin, and the water-displacement method may then be used. After the voids have been determined, a pressure-drop experiment is best performed under controlled flow conditions. Solution for λ is then immediately possible by substituting respective values into equation (12).

For spheres, $\lambda=1$; but for all other particles, $\lambda>1$. This is in agreement with the fundamental observation that a sphere is that shape that provides a given volume with the least surface area.

Two factors seem primarily responsible for the loss of pressure that a compressible fluid suffers when passing through packed columns. They are (1) expansion and contraction caused by the shape of the voids into and through which the fluid must flow and (2) friction between the fluid stream and the particle surface. If beds of equal void content were made up of spheres, cylinders, and rings, the rings, having the largest surface area per unit tower volume, would offer the greatest resistance to the fluid stream. It appears, therefore, that the shape factor merely accounts for the additional effect which the increased surface of nonspherical packings exerts upon the pressure drop.

The validity of the equation was tested over a range of $\frac{D_p}{D_t}$ extending from 0.074 to 0.615. In spite of this considerable variation, no correction factor for wall effect was required in equation (14). The reason for this omission is apparent from an examination of the method by which δ was determined. If δ is found by immersion, the wall effect is accounted for in the measurements. This has already been observed by Carman,[19] and simple proof will be given later. The fact that the equation applies to high ratios of $\frac{D_p}{D_t}$ seems to indicate a fundamental similarity between flow through empty and very loosely packed conduits. For mixed spheres, a satisfactory correlation results when the arithmetic average diameter on a weight basis is chosen for D_p.

Examination of figure 10 indicates that the scatter of the data is approximately ± 8 percent. Experimental measurements may be in error by as much as ± 5 percent, owing to an

[19] Work cited in footnote 36, p. 5.

uncertainty of ±0.5 percent in the determination of the voids in the bed. For this reason, it is believed that the correlation incorporates all of the major variables usually encountered with random packing.

NOMOGRAPH OF PRESSURE-DROP EQUATION

Design of catalytic equipment frequently involves a great number of pressure-drop calculations. As the order of magnitude arising from various operating conditions is the primary factor rather than the high degree of accuracy of the results, an alinement chart may save time for the engineer. Consequently, equation (12) has been used for the construction of a nomograph.

CONDENSATION OF THE EQUATION

Most common gases have viscosities within the range 0.019 to 0.077 lb. hr.$^{-1}$ ft.$^{-1}$. These values, when raised to the 0.1 power as required by equation (12), become 0.73 ±7 percent. As this variation is within the limits of error of the pressure-drop correlation, the value of 0.73 for $\mu^{0.1}$ may be accepted as constant for the purposes of the nomograph. With Δp expressed in pounds per square inch, the constant 3.50 becomes 0.0243. Combining this with g and $\mu^{0.1}$ transforms equation (12) to equation (15).

$$\Delta p = 4.27 \times 10^{-11} G^{1.9} \frac{(1-\delta)}{\delta^3} \left(\frac{\lambda}{D_p}\right)^{1.1} \rho^{-1.0} \quad (15)$$

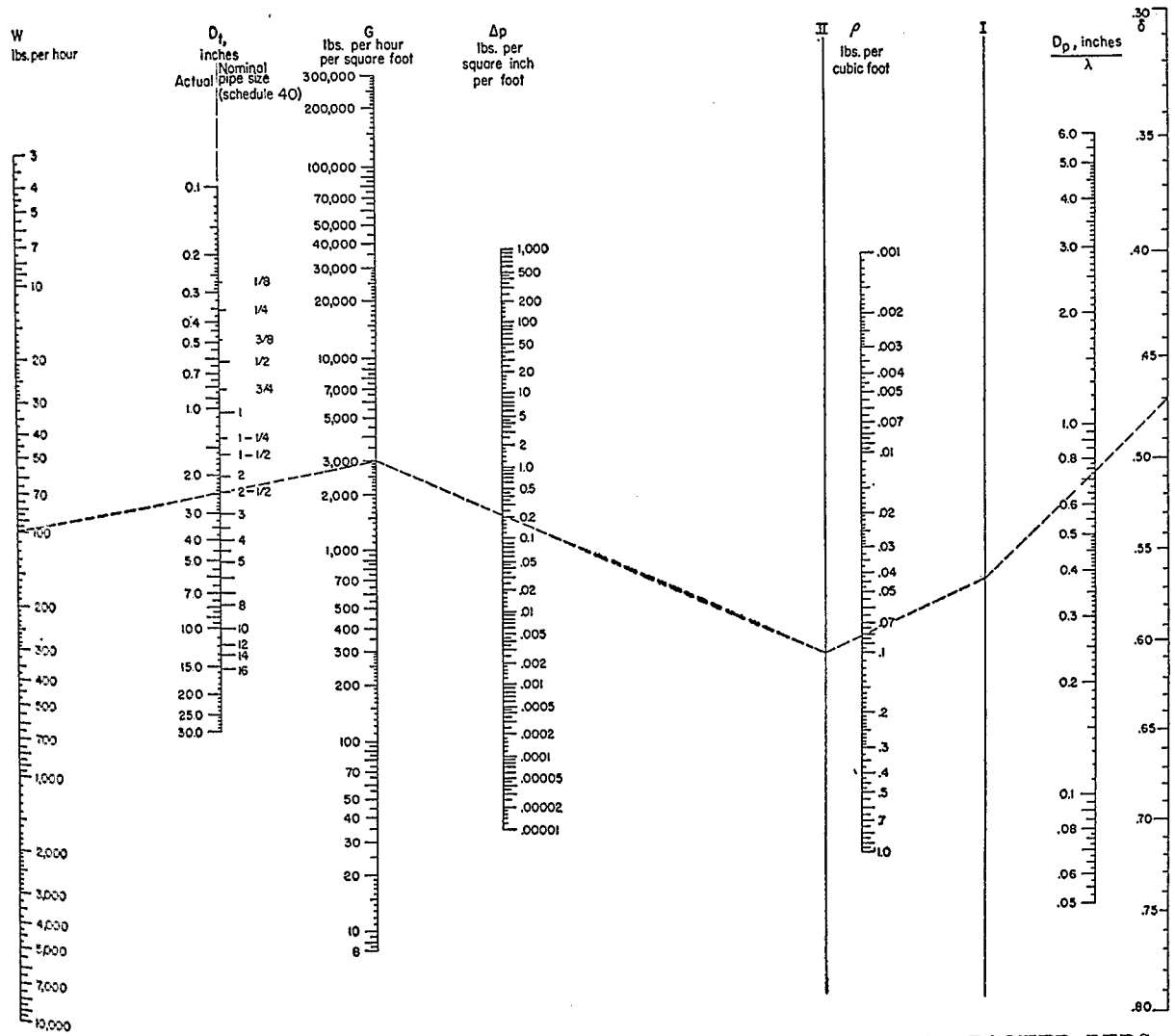

FIGURE 11.—PRESSURE DROP FOR GASES IN TURBULENT FLOW THROUGH PACKED BEDS.

It may be noted that for regular geometric shapes the ratio D_p/λ can be evaluated by the defining equation (9).

$$\lambda=\frac{0.205A}{V_p^{2/3}} \qquad D_p=(6V_p/\pi)^{1/3} \text{ and } \frac{D_p}{\lambda}=6V_p/A.$$

The nomograph (fig. 11) was constructed from equation (15) with an axis for each of the four groups of variables.

ILLUSTRATION

Figure 11 may be used to solve several types of problems.

PROBLEM 1

One thousand pounds of air per hour is to be blown through a reactor consisting of ten 2.5-inch-diameter by 10-foot-long pipes in parallel. The pipes are packed with moderately smooth cylinders 0.740 inch in diameter and 0.740 inch long. It has been determined that 191 cylinders just fill 2 feet of 2.5-inch-diameter pipe. The average air temperature is to be 197° F. Inlet pressure is 5 p.s.i.g.

What pressure drop can be expected?

Solution

The modified Reynolds number is D_pG/μ, approximately 4,400, and hence well in the turbulent range for which the nomograph holds. The volume of each packing particle is:

$$(0.740)(\pi)(0.740)^2/4=0.318 \text{ in.}^3.$$

The particle-surface area is:

$$(\pi)(0.740)^2/2+(\pi)(0.740)(0.740)=2.58 \text{ in.}^2.$$

The volume of 2 feet of 2½-inch-diameter pipe is 114.8 in.^{3}.

The volume of 191 pellets is 60.7 in.^{3}.

$$\delta=\frac{114.8-60.7}{114.8}=0.470.$$

$$\frac{D_p}{\lambda}\frac{6V_p}{A}=\frac{6\times0.318}{2.58}=0.740 \text{ in.}$$

Inlet air density is calculated to be 0.081 lb./ft.^{3}. As a first approximation, assume that the change in gas density as a result of pressure drop is negligible and that 0.081 lb./ft.^{3} is the average density of the gas.

Because the tubes are in parallel, the pressure drop through all the tubes will be equal to that through any one tube. The flow through one tube is:

$$w=1000/10=100 \text{ lb./hr.}$$

Tabulation of values:

$w=100$ lb./hr., $D_t=2.5$ in., $\delta=0.47$,

$\rho=0.081$ lb./ft^3, $D_p/\lambda=0.740$ in.

Use of Nomograph

Connect 100 on the W axis with 2.5 on D_t (nominal) axis and read $G=3{,}000$.

Connect 0.47 on the δ axis with 0.74 on the D_p/λ axis; pivot the straight edge at its intersection with reference line I to cross ρ at 0.081 and intersect reference line II. This last point of intersection is connected with the previously determined value of $G=3{,}000$, and the connecting line is found to cross the Δp axis at the value of 0.22 p.s.i./ft.

The total pressure drop for the 10 feet of pipe will be 2.2 p.s.i. The average pressure in the system will be 5—2.2/2=3.9 p.s.i.g., which will correspond to a gas density 0.945 times that originally assumed. This value will, in turn, lead to a final value of pressure drop of $\frac{2.2}{0.945}$=2.3 p.s.i.

PROBLEM 2

Fifteen thousand pounds per hour of gas at 100 p.s.i. and a density at this pressure of 0.15 lb./ft.^{3} are to be passed through a tower 20 feet tall packed with 1-inch porcelain Berl saddles.

What tower diameter is required to keep the pressure drop below 10 p.s.i.?

Solution

Manufacturer's data provide the following values:

Volume of each particle—0.233 in.^{3}
Area of each particle —4.95 in.^{2}
Voids —69 percent.

From these data,

$$\frac{D_p}{\lambda}=\frac{6V_p}{A}=0.283 \text{ in. and } D_p=0.764 \text{ in.}$$

For a pressure drop of 10 p.s.i., the average pressure will be 95 p.s.i.a., and

$$\rho=(0.15)\ \frac{95}{100}=0.143 \text{ lb./ft.}^3$$

$$w=15{,}000 \text{ lb./hr.}$$

$$\Delta p=10/20=0.50 \text{ p. s. i./ft.}$$

On the nomograph, aline $\delta=0.69$ with $D_p/\lambda=0.283$ inch to find a point on reference I. Aline this point with $\rho=0.143$ lb./ft.^{3} to locate a point on reference II. Alining this point with $\Delta p=0.50$ gives an allowable value of G, 8,600 lb. hr.$^{-1}$ ft.$^{-2}$.

As the value of $w=15{,}000$ does not appear on the nomograph, one may calculate D_t (in feet) from the formula:

$$D_t=\left(\frac{w}{0.785G}\right)^{1/2}.$$

or estimate it from the nomograph by using a value of w equal to one-quarter that specified and taking as an answer for D_t twice the value given by the nomograph. By this latter method, for $G=8,600$, if w were 3,750, D_t would be 8.6 inches, from which the desired value of D_t is 17.2 inches.

The existence of turbulence is now verified by calculation of a modified Reynolds number of 12,200.

EFFECT OF SURFACE ROUGHNESS

Equation (14) is based on data that were observed with smooth particles. From considerations of flow through empty pipes,[20] it is known that roughness of the surface in contact with the moving fluid has a considerable effect upon the pressure drop in the turbulent range. As industrial packing materials rarely are smooth, the effect of surface roughness of particles on the flow of fluids through packed sections was determined. A few orienting tests with very rough materials indicated that the effect is considerable and justified further investigation.

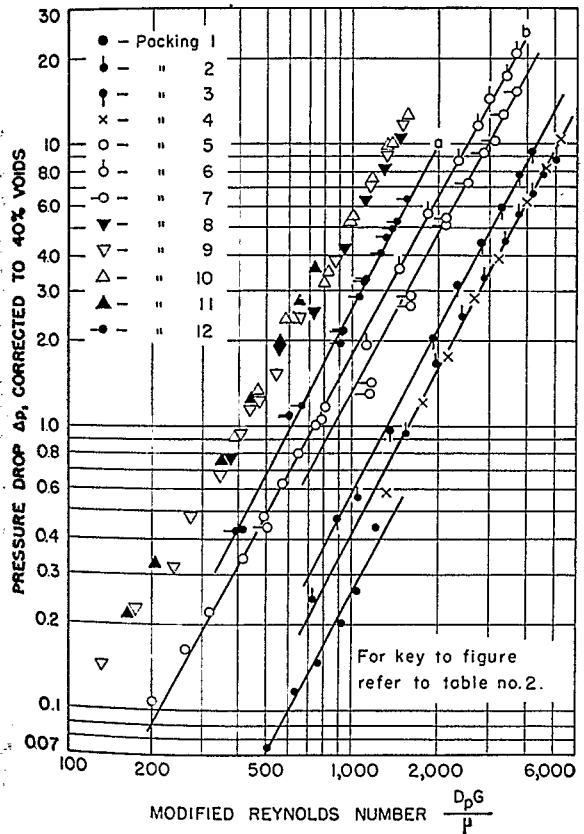

FIGURE 12.—PRESSURE DROP THROUGH COMMERCIAL PACKING MATERIALS.

[20] Nikuradse, J., Verein Deutscher Ingenieure, Forschungsheft 361, 1933.

MATERIALS AND DATA

New data with rough particles are recorded in table II of the appendix. They are shown graphically in figure 12. Figure 13 records data observed by Oman and Watson;[21] their original data are tabulated in table III of the appendix.

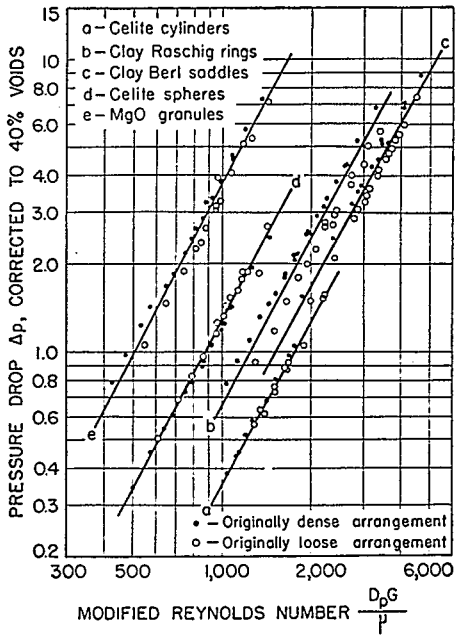

FIGURE 13.—DATA OF OMAN AND WATSON.

Both plots show, on logarithmic coordinates, the pressure drop corrected to 40-percent voids in relation to the modified Reynolds number. Tables 2 and 3, keys to figures 12 and 13, list the general properties of the packings. Materials of different degrees of roughness were used. Representative samples of the pellets originally employed by Oman and Watson [22] were obtained and examined for their surface condition. The celite spheres and celite cylinders were smoothest. They were comparable with the heavy metal oxide pellets supported on kieselguhr, which were described in the section covering the general correlation.

[21] Work cited in footnote 38, p. 6.
[22] Work cited in footnote 38, p. 6.

TABLE 2.—*Properties of packing materials*

Packing	D_p, in.	D_t, in.	$\frac{D_p}{D_t}$	Shape	Nominal dimensions, in.	Shape factor	Material	Original voids in bed, percent	Average gas density, lb./ft.³
1	0. 368	3. 068	0. 120	Spheres		1. 00	Clay	43. 8	0. 0785
2	. 310	. 824	. 376	do		1. 00	do	51. 5	. 0815
3	. 298	. 824	. 362	do		1. 00	do	56. 1	. 0815
4	. 325	1. 049	. 310	do		1. 00	do	51. 7	. 0824
5	. 252	3. 068	. 082	Raschig rings	1/4	1. 50	do	54. 7	. 0761
6	. 252	. 824	. 306	do	1/4	1. 50	do	62. 2	. 0823
7	. 252	1. 049	. 240	do	1/4	1. 50	do	61. 2–57. 0	. 0830
8	. 170	. 824	. 206	Rounded granules		1. 10	Aloxite	54. 2–55. 6	. 0834
9	. 165	3. 068	. 054	Sharp granules		1. 10	do	54. 0	. 0760
10	. 170	. 824	. 206	do		1. 10	do	57. 3–58. 0	. 0830
11	. 159	2. 067	. 077	do		1. 10	do	54. 4	. 0837
12	. 180	. 824	. 218	Cylinders	3/16	1. 15	Alundum	48. 5–44. 7	. 0845
								44. 2	

TABLE 3.—*Properties of packing materials used by Oman and Watson*

Packing	D_p, in.	D_t, in.	$\frac{D_p}{D_t}$	Shape	Nominal dimensions, in.	Shape factor	Material	Original voids in bed, percent
a	0. 333	4. 026	0. 083	Cylinders	1/4	1. 16	Celite	36. 1–46. 1
b	. 400	4. 026	. 099	Raschig rings	3/8	1. 90	Clay	55. 45–62. 3
c	. 480	4. 026	. 119	Berl saddles	1/2	2. 50	do	71. 05–76. 35
d	. 217	4. 026	. 054	Spheres	1/4	1. 00	Celite	37. 75–46. 9
e	. 1875	4. 026	. 047	Granules	3/16	1. 1	MgO	42. 5–51. 6

The Raschig rings of the present work, as well as those employed by Oman and Watson, consisted of ordinary commercial clay. The surfaces were unglazed and dull. Fine protuberances could be observed on the material, and the roughness was barely noticeable when the particles were moved gently over the skin. The roughness of the clay balls and the Berl saddles seemed approximately equal to that of the Raschig rings.

The Alundum cylinders appeared a trifle rougher, and the roughness seemed sharper than that of the clay particles. The particle density of these cylinders was determined by water immersion.

The Aloxite granules possessed sharp corners and were very much rougher than the materials previously discussed. The particles resembled coke and were somewhat vesicular. Comparatively large pores could be observed on the surface, and upon immersion in water the material absorbed a considerable amount, releasing the entrapped air in the form of fine bubbles. This property interfered considerably with the determination of voids in the beds. Obviously, water immersion would have given high values of δ. Presaturation of the material with water was not too satisfactory and gave poor check results. A reliable procedure finally was adopted, which consisted in soaking a weighed quantity of Aloxite granules in molten stearic acid, permitting the excess stearic acid to drip off the surface, and determining the displacement volume of the granules thus treated in water. This method yielded an apparent density of 2.0 g./cc. This value was used for the void determinations.

The magnesium oxide granules used by Oman and Watson [23] were not quite so rough as the Aloxite particles, although a considerable number closely approached the Aloxite particle condition. The magnesium oxide granules, however, were much rougher than the clay and Alundum particles. They also possessed the sharp corners that differentiated the Aloxite particles distinctly from the other materials. These sharp corners were the subject of a special investigation. One batch of the Aloxite was charged into a ball mill and "ground round." This treatment merely rounded off the corners but left the surface roughness intact. No mealy material adhered to the surface. After this milling operation, the Aloxite particles were chiefly egg-shaped and ellipsoid; a few of the

[23] Work cited in footnote 38, p. 6.

particles resembled disks, and a small number were almost spherical. Packing No. 8, described in table 2, represented this rounded material. Packing No. 10, the original sharp Aloxite granules, as well as the rounded bodies were investigated in a tube with D_t=0.824 inch, and the results shown in figure 12 indicate that the data obtained with packing No. 8 agree with those of packing No. 10. From this observation it was concluded that rounding off the corners had no significant effect upon the pressure drop.

CORRELATION

Figures 12 and 13 show that the pressure drop is proportional to $Re^{1.9}$ and also to

$$\frac{(1-\delta)}{\delta^3}.$$

It seems, however, that these data were not as reproducible as the measurements reported with smooth materials.

The range of the data in the present paper, as far as the ratio of particle to tube diameter is concerned, was quite large. D_p/D_t varied from 0.047 to 0.376. The percentage of voids in the various beds ranged from 36.1 percent for the celite cylinders of Oman and Watson to 76.35 percent for the Berl saddles of the same investigators. This is an impressive variation, and its effect upon the pressure drop will be discussed in greater detail.

Packings 8, 9, and 10 each consisted of a sized fraction of Aloxite greater than 0.157 inch in diameter but smaller than 0.185 inch. The geometric mean of the two sieve openings was chosen as D_p. The composition of packing No. 11 is shown in table 4. The choice of a proper value for D_p under conditions of mixed sizes was stressed earlier. To find D_p for granules, geometric mean sizes were calculated from adjacent sieve openings, and these values were averaged arithmetically on a weight basis.

TABLE 4.—*Size distribution of packing No. 11*

Sieve openings, inch	Weight-percent	D_p of fractions, inch	(Weight-percent) × (D_p of fractions) / 100
0.250	0. 06	0. 250	0. 0002
.250–.185	3. 50	. 215	. 0075
.185–.157	57. 00	. 170	. 0968
.157–.132	33. 90	. 144	. 0488
.132–.111	3. 50	. 121	. 0042
.111–.093	. 40	. 101	. 0004
.093	1. 64	. 093	. 0015
		D_p of mixture=0.1594	

In view of the numerous modes of packing arrangements possible when granules are dumped into 0.75-inch, 2-inch, and 3-inch pipes, the data on the Aloxite are in good agreement.

In figure 14, modified friction factors for the various materials were plotted against modified Reynolds numbers using logarithmic coordinates. Frictions factors were obtained by solving equation (14) for f. For the Aloxite and magnesium oxide granules, a shape factor of 1.1 was assumed; this value is correct for

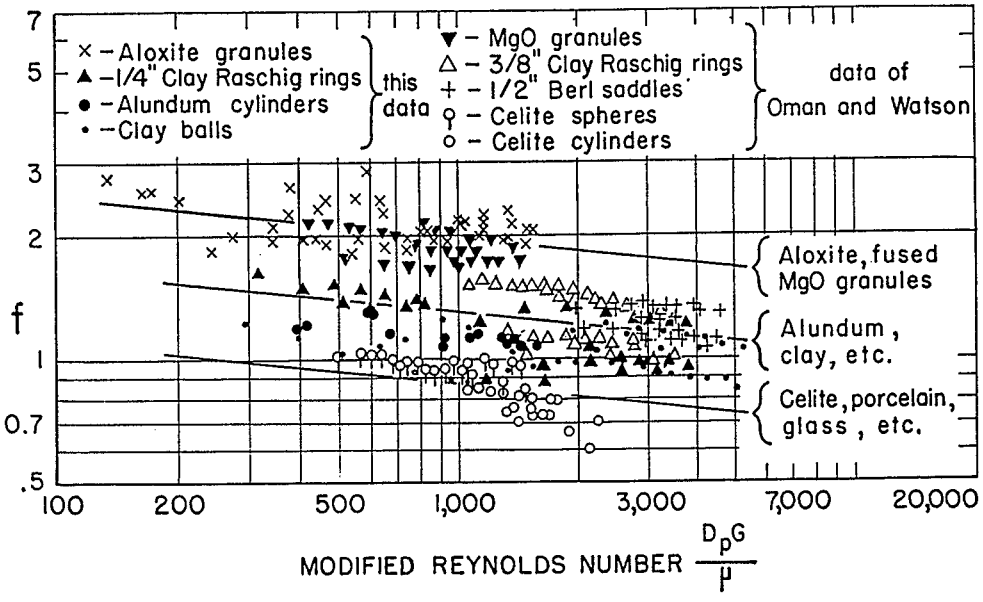

FIGURE 14.—FRICTION FACTORS FOR VARIOUS MATERIALS.

particles having a shape halfway between spheres and octahedrons. For the Berl saddles, the shape factor was calculated from the manufacturer's data; the method of calculation will be discussed later. For all the other shapes, λ was calculated from the average dimensions of the particles. Figure 14 shows the marked effect of surface roughness, as shown by the data arranged into three distinct groups. The lowest group with the smallest friction factors pertains to the smoothest particles, that is, the celite spheres and cylinders. All data discussed earlier fell into this general region. The line drawn through the celite particle data is the same as that laid through the smooth data shown in figure 10. Immediately above this group is another pertaining to the clay and Alundum particles. There is slight "diffusion" of the data of the second group into those of the lower group. This is to be expected in view of the experimental error. Another friction-factor line was drawn through this second group. The slope of the second line is the same as that of the first, lower line. Above the second group is another group comprising the data of Aloxite and magnesium oxide granules. As these granules were much rougher than the other particles, it is not surprising to find these data rather sharply separated from the data pertaining to the clay and Alundum particles. A friction-factor line parallel to the two lower lines was drawn through these points.

Because all three friction-factor lines could be drawn in with the same slope, it was concluded that the degree of surface roughness has no effect upon the factor for the state of flow, which equals 1.9 for this range of turbulence.

The expressions for the three friction-factor lines are:

$$f=\frac{1.75}{Re^{0.1}}, \text{ for smooth particles such as glass, porcelain or celite:} \quad (13)$$

$$f=\frac{2.625}{Re^{0.1}}, \text{ for clay and Alundum;} \quad (16)$$

and

$$f=\frac{4.0}{Re^{0.1}}, \text{ for Aloxite and MgO granules.} \quad (17)$$

When these expressions for f are substituted into equation (14), one obtains:

$$\Delta p=\frac{3.50G^{1.9}\mu^{0.1}\lambda^{1.1}(1-\delta)}{D_p^{1.1}g_c\rho\delta^3}, \text{ which is equation (12) and valid for smooth particles.}$$

$$\Delta p=\frac{5.25G^{1.9}\mu^{0.1}\lambda^{1.1}(1-\delta)}{D_p^{1.1}g_c\rho\delta^3}, \text{ which is valid for clay, Alundum, and other similarly rough particles.} \quad (18)$$

$$\Delta p=\frac{8.0G^{1.9}\mu^{0.1}\lambda^{1.1}(1-\delta)}{D_p^{1.1}g_c\rho\delta^3}, \text{ which is valid for Aloxite, MgO granules, and other types of similarly rough granules.}$$

(19)

DISCUSSION OF RESULTS

It is difficult to describe surface roughness of particles. To define the degree of roughness by the average height of the protuberances on the surface is probably not enough. Nikuradse [24] has experimented with flow of fluids through pipes of varying roughness. He defined the degree of roughness by an index of the form $\frac{e}{r_t}$, where e is the average height of the protuberances on the pipe surface and r_t is the radius of the pipe. The ratio of e/r_t is referred to as relative roughness. It seems plausible that the roughness of particles could be defined by a similar index, and r_p would then be the equivalent particle radius. A relationship pertaining to packing materials could possibly be developed between the pressure drop and a quantity such as e/r_p; this was not attempted, because roughness data are not ordinarily available from equipment-design specifications. If manufacturers of packing materials accompanied their data with roughness indexes, it would be practical to study the problem more precisely. Until such information is available, it is necessary to describe surface roughness in this comparative manner.

Referring to figure 14, it appears that the pressure drop through packed beds is approximately doubled when the degree of surface roughness is increased from that represented by celite to the roughness of Aloxite granules. This relationship probably has not yet been recognized in a quantitative sense, chiefly because the severe influence of the voids upon the pressure drop through packed beds was not sufficiently well appreciated. When smooth cylinders are dumped into a tube, the normal voidage of the resulting bed is approximately 12 percent smaller than when very rough granules of approximately equal size are dumped into the same tube. If the cylindrical bed contains 43 percent and the granular bed 55 percent voids, for equal mass flows and equal packing heights the ratio of the pressure drop through the bed of cylinders, Δp_c, as compared to the pressure drop through the granular bed, Δp_g, would be approximately

$$\frac{\Delta p_c}{\Delta p_g}=\frac{(1-0.43)(0.55)^3}{(0.43)^3(1-0.55)(2.28)}=1.16,$$

where the factor 2.28 in the denominator accounts for the effect of the rough surface. This indicates that under these packing conditions the pressure drop through the smooth cylinders is 1.16 times that through the much rougher granular bed.

[24] Work cited in footnote 20, p. 17.

It was mentioned previously that the densest bed considered in this study contained 36.1 percent voids. This bed consisted of celite cylinders. The equivalent spherical diameter of these pellets was 0.333 inch, and the calculated shape factor was 1.16. In contrast, the least dense bed, consisting of 0.5-inch clay Berl saddles contained 76.35 percent voids. The equivalent spherical diameter of the saddles as calculated from the manufacturer's data was 0.48 inch, and the shape factor was 2.5. For equal mass flows, gas densities, and packing heights, the actual pressure drop through the cylinders, Δp_c, as compared with the actual loss through the saddles, Δp_s, would be approximately

$$\frac{\Delta p_c}{\Delta p_s}=\frac{(1-\delta_c)\delta_s{}^3\lambda_c{}^{1.1}D_{ps}{}^{1.1}}{\delta_c{}^3(1-\delta_c)\lambda_s{}^{1.1}D_{pc}{}^{1.1}(1.5)}=\frac{(1-0.361)(0.7635)^3(1.18)(0.446)}{(0.361)^3(1-0.7635)(2.74)(0.298)(1.5)}=11,$$

wherein subscript c refers to cylinders and subscript s to saddles. The factor 1.5 in the denominator accounts for the roughness effect of clay as compared with celite. The result indicates that under these conditions the pressure drop through the smooth cylinders is 11 times that through the comparatively rough, clay saddles. A variation in voids from 76.35 to 36.1 percent, all other variables remaining constant, would multiply the pressure drop by

$$\frac{(1-0.361)(0.7635)^3}{(0.361)^3(1-0.7635)}=25.4;$$

whereas, changing from clay to celite would decrease Δp only by

$$100\left(1-\frac{1}{1.5}\right)=33 \text{ percent.}$$

These simple considerations demonstrate to what extent surface roughness and bed voidage affect pressure drop. The influence of surface roughness would not have been recognized if the pronounced effect of the voids upon the pressure drop had not been considered quantitatively first.

Proof has been presented earlier that in the turbulent range it is sufficiently accurate to consider the pressure drop proportional to $(1-\delta)/\delta^3$ rather than to $(1-\delta)^{1.1}/\delta^3$. For a comparatively small variation in percentage voids (for example, from 35 to 45 percent), the error is negligible. When the percentage of voids ranges between 36.1 and 76.35, as in the present study, the error introduced is somewhat larger; but, even for this wide variation in the porosity of the bed, the discrepancy is still within the limits of the experimental error.

General belief has been that the chief reasons for fluid pressure drop in packed columns are losses due to expansions and contractions in the case of compressible fluids and changes in velocity head when dealing with noncompressible fluids. Only an insignificant portion of the pressure drop was believed to be a result of surface conditions. Orientation studies made by Martin [25] indicate that a definite fraction of the pressure drop is caused by expansions and contractions; this is substantiated by the pronounced effect that fractional voids have on the pressure drop. However, the data of this study indicate that the surface condition also is important. This is clearly demonstrated by the significant increase in pressure drop when proceeding from smooth particles, such as glass, to very rough granules. In this particular case the maximum increase is 2.28-fold. Brownell and Katz [26] have proposed a data correlation that also includes surface roughness as one of the variables. They recorrelated data from the literature in addition to some of their own data and, by a suitable choice of parameters, superimposed the data on a standard Moody friction-factor plot for flow through empty conduits. They assigned roughness indexes, e/r_p, to the individual materials and thus showed a plot similar to that given in figure 14. Consideration of their data in the turbulent range shows, roughly, a spread of 100 percent, indicating a maximum roughness multiplication factor of approximately 2.

It is instructive to compare figures 14 and 15. In figure 15, the logarithms of friction factors are plotted against the logarithms of Reynolds numbers for fluid flow through empty pipes of

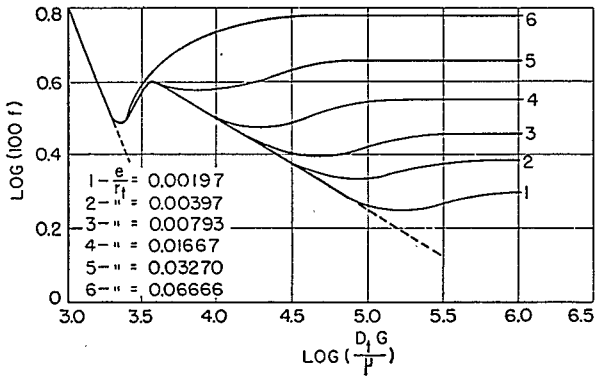

FIGURE 15.—VARIATION OF FRICTION FACTOR WITH REYNOLDS NUMBER FOR FLOW THROUGH EMPTY PIPES OF DIFFERENT DEGREES OF ROUGHNESS (ACCORDING TO NIKURADSE).

[25] Martin, J. J., D.Sc. Thesis in Chem. Eng.: Carnegie Inst. of Tech., 1948.

[26] Work cited in footnote 39, p. 6.

various degrees of roughness. These curves represent actual data obtained by Nikuradse,[27] and friction factors for flow through empty pipes increase with increasing roughness of the interior pipe surface. Figure 14 is strictly analogous to figure 15. However, Nikuradse investigated a much larger flow range than was studied in this research.

It was pointed out earlier that the roughness of particles may, perhaps, be expressed quantitatively by the index e/r_p. For extremely rough particles the quantity e, the average height of the surface protuberances, would be comparatively high and would eventually approach the order of magnitude of the particle radius. Such rough surfaces would greatly affect the ratio of

$$\frac{\text{particle surface area, } A}{\text{particle volume, } V_p}.$$

As the shape factor, λ, is a function of A/V_p, a fundamental relationship may exist between roughness and shape factor. For such extremely rough particles it would be difficult to decide, therefore, whether it is the increased roughness or the shape factor that affects the pressure drop.

PREDICTION OF VOIDS IN PACKED TUBES

Earlier discussions have stressed the important effect of the voidage upon the resistance to flow through beds of broken solids. Pressure drop was shown to be proportional to an expression of the form

$$\frac{(1-\delta)^{3-n}}{\delta^3},$$

which, for highly turbulent flow, becomes

$$\frac{(1-\delta)}{\delta^3}.$$

All other variables in the equation remaining constant, a change in fractional voids from 0.40 to 0.50 reduces the pressure drop more than 50 percent. As designers of new equipment usually have only vague ideas about the apparent density of the packing materials to be used, the uncertainty thus introduced in calculations from equation (14) makes the development of a simple correlation for fairly accurate estimation of the fractional voids in packed vessels desirable. To make the relationships useful for general engineering design, it was attempted to include only such quantities in the correlation as are ordinarily available from equipment and process specifications.

[27] Work cited in footnote 20, p. 17.

METHODS OF CHARGING VESSELS

In industrial practice there are three chief methods of charging packed vessels:

1. Stacking of individual packing elements in the vessel.
2. Dumping the packing into vessels filled with water and subsequently drawing off the water.
3. Dumping the packing into the empty vessels.

The first method is never used with granules or small, irregularly shaped particles. It is commonly used with comparatively large geometrical shapes, where, for the sake of definite process advantages, a certain arrangement of the elements is desired. This method provides an exact means of evaluating the percentage of voids in the bed, because the number of pieces used is generally known.

The second method is employed where it is desired to have a comparatively loose bed. Gradual settling of the particles in the loose bed, however, chiefly as a result of mechanical vibrations in the plant, eventually increases the packing density. Moreover, there are a great number of materials, especially process catalysts, that are permanently impaired if submerged in water or other fluids. For these reasons this method of charging also is comparatively rare.

The conventional procedure is to dump the packing into the open vessels. This method usually does not produce the densest bed; however, the bed gradually settles by virtue of its own weight and mechanical vibrations from the environment. Eventually, a condition of "practical maximum bed-density" is approached, which is a safe condition upon which to base a design. This explains why the vessels used in the experimental work described in this section were charged by "dumping" and "dumping and pounding."

VARIABLES

The chief variables believed to influence the packing density and percentage of voids in a bed are:

a. Particle diameter (diameter of the sphere of equivalent volume).
b. Tube or vessel diameter.
c. Particle-size distribution.
d. Particle shape.
e. Particle-surface roughness.
f. Method of charging.
g. Specific gravity of packing particles.

EXPERIMENTAL DETAILS

The vessels used for this work were pipes 30 inches long, welded shut at one end. Table IV of the appendix lists the original experimental

data. Table 5 shows the orientation of the work and the physical properties of the packing material. The packing materials were dumped into the vessels in a slow, steady stream. In no case could the results of this dumping procedure be duplicated precisely. The average deviation between check runs (about ±1 percent) was not significant, however.

TABLE 5.—*Summary of experimental runs*

Packing	Material	Shape	D_p, inch	Nominal standard pipe in which voids were determined	Remarks
a	Glass	Spheres	0.172	¾, 1, 1¼, 2, 3, 4	Smooth surface, uniform sizes (fig. 16).
b	do	do	.228	¾, 1, 1½, 2, 3, 4	
c	do	do	.338	¾, 1, 1½, 2, 3, 4	
d	do	do	.5075	¾, 1, 1½, 2	
e	Steel	do	.437	1	
f	Porcelain	do	.730	1½, 2, 3, 4	
g	Glass	do	.200	1½, 2, 3, 4	Smooth surface mixed spheres. For compositions, see table 6 (fig. 17).
h	do	do	.298	1½, 2, 4	
i	Glass and porcelain	do	.386	1½, 2, 3, 4	
j	do	do	.536	1½, 2, 3, 4	
k	Glass	do	.208	¾	
l	do	do	.271	¾	
m	Glass and porcelain	do	.323	¾	
n	Clay	do	.325	¾, 1, 1¼	Moderately rough surface (fig. 18).
o	do	do	.368	1½, 2, 3, 4	
p	Cobalt oxide	Cylinders	.466	½, ¾, 1, 1½, 3, 4	Smooth surface (fig. 19).
q	Aluminum	do	.254	½, ¾	
r	Copper	do	.274	½, ¾, 1	
s	Chromium oxide	do	.239	½, 1, 4	
t	Alundum	do	.180	¼, ⅜, ½, ¾, 1, 1½, 2, 3.	Rough surface [1] (fig. 20).
u	Clay	Rings	.252	⅜, ½, ¾, 1, 1½, 2, 3, 4.	Commercial Raschig rings moderately rough surface (fig. 24).
v	Clay	do	.397	¾, 1, 1½, 2, 3, 4	
w	Aloxite	Granules	.1219	½, ¾, 1	Rough surface (fig. 21).
			.1511		
			1.469		
x	Iron oxide	do	.0898	½, ¾, 1	Rough surface (fig. 22).
			.1058		
			.1418	1.469	
			.2054		
y	Alundum	do	.0732	½, ¾, 1	Fused, rough granules (fig. 23).
			.1007		
			.1601	1.469	

[1] Cylinders, 3.8 mm. diameter × 5 mm. high.

After the vessels had been charged with a known (solid) volume of particles and the voids had been determined from the packed height and the inside diameter of the vessel, the packed column was pounded on the outside with a hammer for approximately 10 minutes—long enough to produce a maximum packing density. The column height was recorded for this denser condition, and the voids were calculated. By adopting this procedure, actual plant conditions were simulated. Correlations of results are shown in figures 16 to 24. The percentage voids of "dumped" and "dumped and pounded" beds, hereafter referred to as "loose" and "dense" beds, respectively, was plotted against the ratio D_p/D_t. Carman [28] used a similar method of correlation for spheres. Cartesian coordinates were used, and, for the materials investigated, D_p/D_t ranged from approximately 0.04 to 0.50. In view of the variety of materials considered, the correlations are satisfactory. The difference between the voids contained in the loose and dense beds was approximately 2 to 5 percent. The curves shown in figure 25 were obtained from the data of figures 16 to 24 by plotting the arithmetical average between the loose and dense arrangements. With the exception of the Raschig rings, all the curves show a general tendency to converge near $D_p/D_t=0$.

[28] Work cited in footnote 36, p. 5.

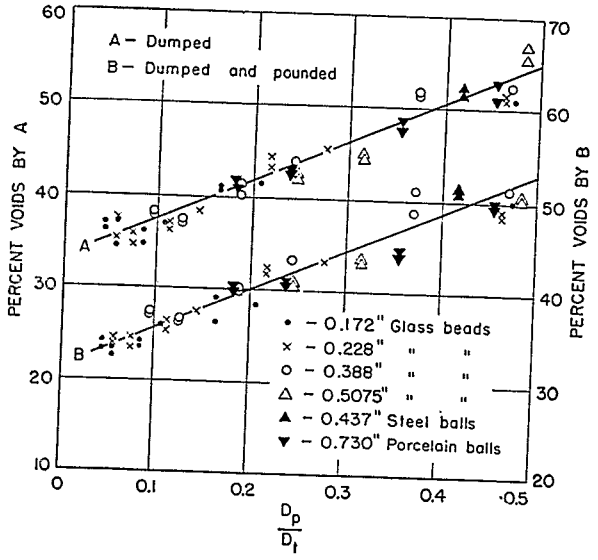

FIGURE 16.—VOIDS IN PACKED TUBES VS. $\frac{D_p}{D_t}$ FOR SMOOTH, UNIFORM SPHERES.

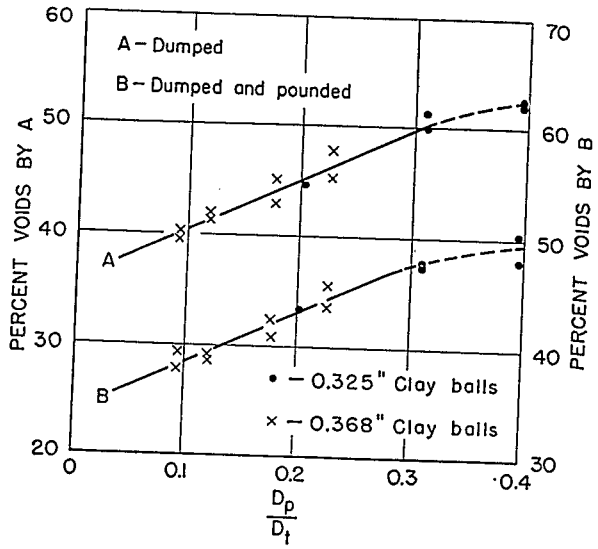

FIGURE 18.—VOIDS IN PACKED TUBES VS. $\frac{D_p}{D_t}$ FOR CLAY BALLS.

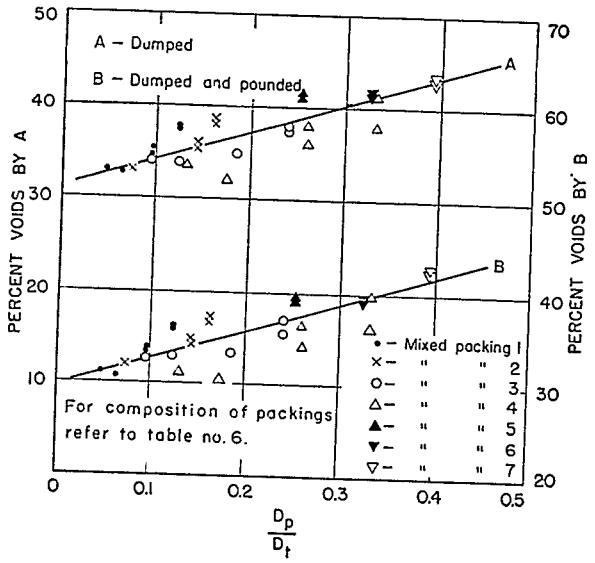

FIGURE 17.—VOIDS IN PACKED TUBES VS. $\frac{D_p}{D_t}$ FOR SMOOTH, MIXED SPHERES.

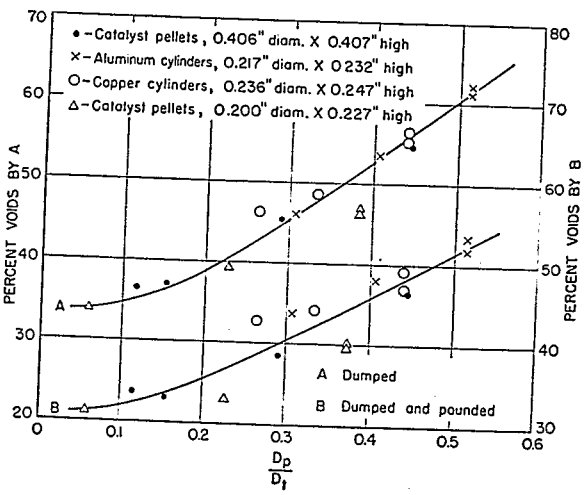

FIGURE 19.—VOIDS IN PACKED TUBES VS. $\frac{D_p}{D_t}$ FOR SMOOTH CYLINDERS.

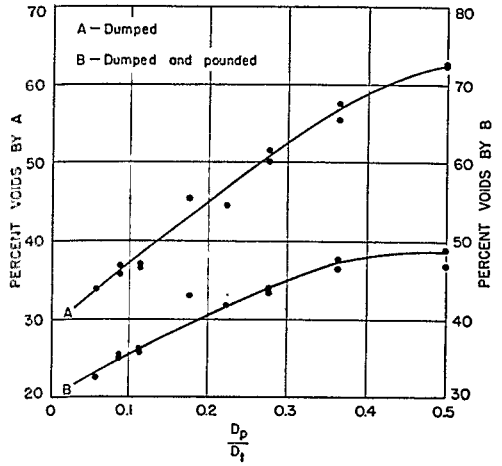

FIGURE 20.—VOIDS IN PACKED TUBES VS. $\frac{D_p}{D_t}$ FOR ALUNDUM CYLINDERS.

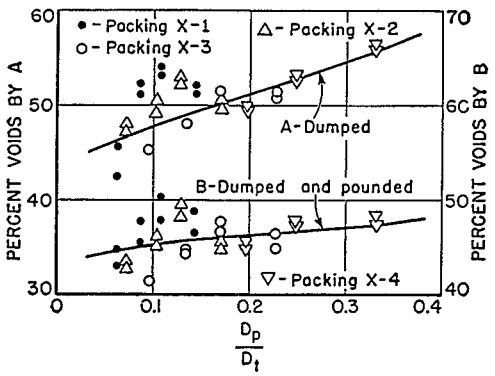

FIGURE 22.—VOIDS IN PACKED TUBES VS. $\frac{D_p}{D_t}$ FOR Fe_3O_4 (IRON FISCHER-TROPSCH CATALYST) GRANULES.

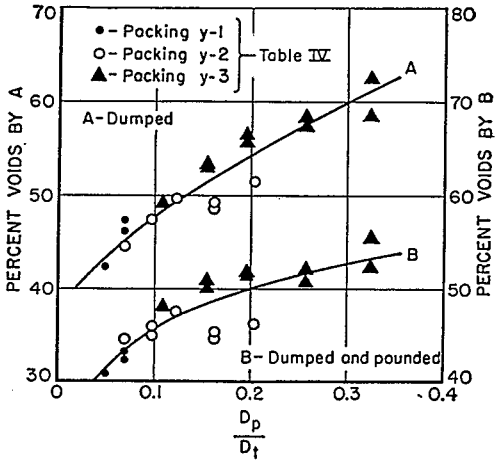

FIGURE 23.—VOIDS IN PACKED TUBES VS. $\frac{D_p}{D_t}$ FOR FUSED ALUNDUM GRANULES.

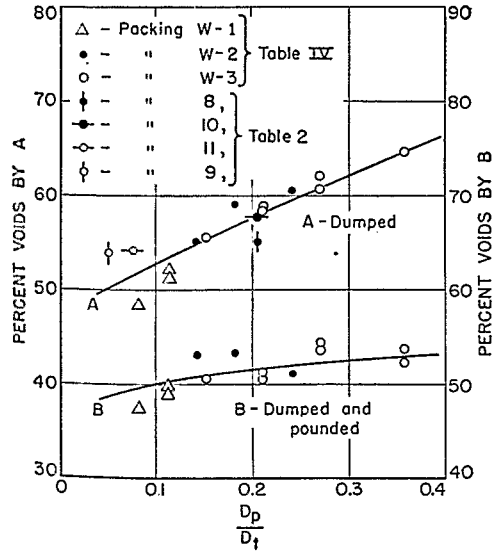

FIGURE 21.—VOIDS IN PACKED TUBES VS. $\frac{D_p}{D_t}$ FOR ALOXITE GRANULES.

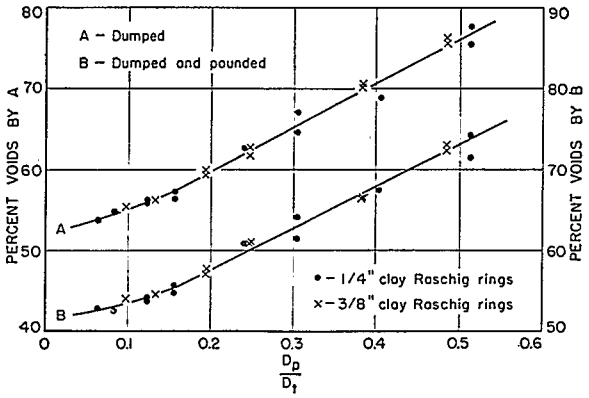

FIGURE 24.—VOIDS IN PACKED TUBES VS. $\frac{D_p}{D_t}$ FOR RASCHIG RINGS.

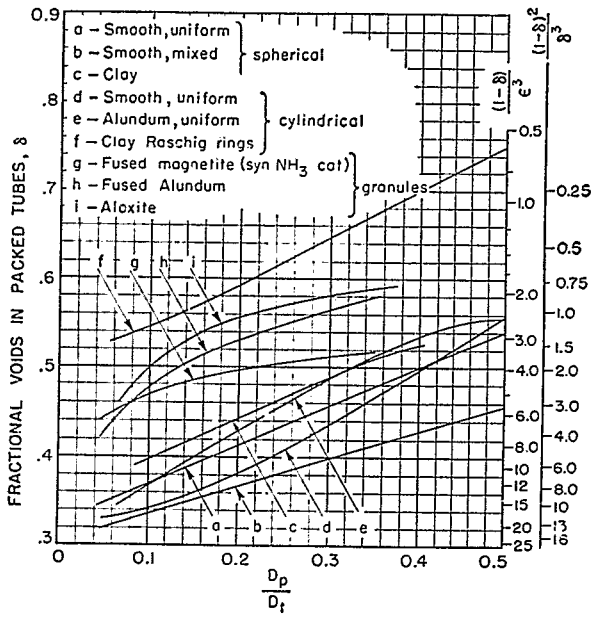

FIGURE 25.—VOIDS IN PACKED TUBES VS. $\frac{D_p}{D_t}$ FOR A VARIETY OF MATERIALS.

COMMENTS

Figure 16 shows data obtained with smooth glass, porcelain, and steel balls. It is important to note that the data referring to the steel balls agree with the rest of the observations. This indicates that, for this method of charging, the material density of the particles has no effect upon the bed voidage, and the problem is simplified. Figure 19 confirms this conclusion and extends it to cylindrical packing particles.

Data referring to mixed spherical packings are presented in figure 17. Deviations of the data from a straight line are greater than those of the data pertinent to uniform sizes shown in figure 16. Figure 17 shows that beds composed of mixed spherical packings are denser than those consisting of uniform spherical particles, provided the methods of bed preparation are comparable. This is in agreement with the observations of Furnas.[29] The reason for the greater bed density obtained with mixed sizes is that the small particles tend to fill the voids between the larger ones.

The compositions of the various mixed packings are recorded in table 6. Packings 1 and 5 consisted of two components, packings 2 and 6 of three components, and packings 3, 4, and 7 of four components. For mixed packing materials, it was pointed out earlier that satisfactory results were obtained when the arithmetic average diameter on a weight basis was chosen for D_p. This may be expressed by:

$$D_p=(Xd_p)_1+(Xd_p)_2+\cdots(Xd_p)_Z, \qquad (20)$$

where X=weight fraction of any component, d_p=equivalent spherical diameter of any component, and subscripts 1, 2, . . . Z refer to the number of components. This convention, when used to calculate D_p/D_t for the various mixtures in figure 17, produced satisfactory results.

TABLE 6.—*Composition of mixed spherical packings*

Mixed packing	D_p of fractions, inch	Volume, percent	Volume percent × D_p of fractions / 100, inch	D_p of mixture, inch	Packing (see table 5)
1	0.172	50.70	0.0873	0.200	g
	.228	49.30	.1122		
2	.172	23.35	.0401	.298	h
	.228	24.74	.0569		
	.388	51.90	.2010		
3	.172	16.55	.0285	.386	i
	.228	15.15	.0346		
	.388	19.85	.0771		
	.5075	48.45	.2458		
4	.172	12.80	.0220	.536	
	.388	18.20	.0706		
	.5075	27.00	.1370		
	.730	42.00	.3064		
5	.172	38.0	.0665	.208	k
	.228	62.0	.1412		
6	.172	30.8	.0530	.271	l
	.228	32.4	.0740		
	.388	36.8	.1440		
7	.172	20.9	.360	.323	m
	.228	17.2	.0393		
	.388	21.6	.0438		
	.5075	40.3	.2040		

Figure 18 presents values observed with clay balls. The curve representing these data is parallel to and above the line referring to the smooth, uniform spheres. The deviation between the two graphs is about 3 percent for the entire range. This is significant because it indicates that rough particles pack less densely than smooth ones under comparable charging conditions. This behavior can be explained as follows: When particles are dumped into a vessel, they normally come to rest when they touch one another and form a stable arrangement. If a temporary unstable arrangement should result, then, under the application of a sufficient force, this arrangement will change to a more stable condition—that is, to a denser bed. Whether the acting force is sufficient to bring about such a change depends on the friction that results when the individual particles move into the more stable position. Because friction is greater between rough particles than between smooth ones, rough particles come to rest sooner when dumped into a tube; the result is a less dense bed. This general behavior is characteristic not only of spherical particles but also of other shapes. Curves *d* and *e* in

[29] Work cited in footnote 33, p. 5.

figure 25 refer to smooth and rough cylinders, respectively. The data pertaining to the comparatively rough Alundum cylinders are above those referring to the smooth cylinders. Deviation between the two lines varies from 2 to 5 percent.

Data referring to cylindrical pellets are shown in figure 19. The correlation is fair. For the pellets used, the ratio of height/diameter ranged between 1.00 and 1.14. Packing *s*, the catalyst pellets, was rounded on top and bottom, whereas all the other particles were true cylinders. Although one would expect these factors to influence results, no significant trend is indicated by the data.

Figure 20 shows results obtained with Alundum cylinders of one size. The reason for the upward convex curvature of these curves, as compared with the upward concave shape of the curves in figure 19 (pertaining to smooth cylinders), is not known. For figures 19 and 20, the diameter of the equivalent volume sphere of the particles was chosen for D_p.

In industrial catalysis, granules are, perhaps, used more frequently than any other particle shape, chiefly because they are cheaper to prepare than particles of cylindrical, spherical, or any other definite shape. Although this is a good reason for using granules, it is not necessarily true that granules are to be preferred for every use. This will be discussed in more detail in a later section.

In figures 21 to 23, data are reported that pertain to some typical granular materials. Data previously discussed indicate that the physical characteristics of the materials, such as shape and surface roughness, have a profound effect upon packing density. As a great number of granules of different types are in commercial use, it was impossible to investigate many for specific reasons. Examination of the data reveals that the Aloxite particles (fig. 21), having the greatest surface roughness, produce a bed of least density. The particle shape factor had been estimated earlier and accepted as $\lambda=1.10$.

Figure 23 shows that the Alundum particles pack more densely in accord with the lesser surface roughness. No shape-factor measurements were made; however, comparison of the particles with the sand particles described later suggests an approximate shape factor of $\lambda=1.5$.

The iron Fischer-Tropsch catalyst granules had little, if any, surface roughness. The data recorded in figure 22 show that the packing density observed with this material is much higher than the other types of granules. The particle shape was very similar to that observed with finely ground catalyst particles and was, therefore, accepted as $\lambda=1.73$.

943247°—51——3

The data of figure 24 refer to two sizes of Raschig rings and seem in good agreement. Owing to the hollow nature of this packing, one would expect a high value for δ. For the Raschig rings, the diameter of the equivalent volume sphere was chosen for D_p. The rings considered in this study were comparatively small. For larger pieces, that is, larger than 0.25 or 0.375 inch, the ratio of inside/outside diameter increases, resulting in a general increase of voids. In view of this fact, it is felt that additional data would be desirable for more accurate work in order to predict the voids present in beds of larger Raschig rings. From a knowledge of the dimensions of the larger pieces, it is possible, however, as the following considerations will show, to estimate the voids present by using the curves shown in figure 25 for cylinders. If curve *f* in figure 25 is employed for larger pieces, a conservative estimate of the pressure drop should result.

GENERAL ESTIMATION OF VOIDS FOR RINGS

Consider a 2-inch standard pipe packed 36 inches high with clay cylinders 0.385 inch in diameter and 0.397 inch high. The voids in a bed packed with clay rings 0.385 inch o. d. × 0.218 inch i. d. × 0.397 inch high may be calculated as follows:

Volume of one cylinder: $(0.385)^2(0.785)(0.397)=0.0461$ in.^{3}

$$D_p=\sqrt[3]{\frac{0.0461\times 6}{\pi}}=0.446 \text{ in.}$$

$$\frac{D_p}{D_t}=\frac{0.446}{2.067}=0.216.$$

From figure 25, $\delta=0.440$ (Alundum cylinder curve):

Solid volume of cylinders in packed columns: $(2.067)^2(0.785)(36)(0.56)=67.5$ in.^{3}

Void volume: $\frac{(67.5)(0.44)}{0.56}=53.0$ in.^{3}

Total column volume: $67.5+53.0=120.5$ in.^{3}

Number of cylinders in packed columns:

$$\frac{67.5}{0.0461}=1{,}470.$$

Assuming that a column packed with rings of the above dimension also contains 1,470 pieces, then:

Volume of one ring:

$$0.0461-(0.2178)^2(0.785)(0.397)=0.0313 \text{ in.}^3$$

$$D_r=\sqrt[3]{\frac{0.0313\times 6}{\pi}}=0.393 \text{ in.}$$

Total solid volume of rings in packed column: $(0.0313)(1470)=46.0$ in.^{3}

Void volume: $120.5-46=74.5$ in.^{3}

$$\delta=\frac{74.5}{120.5}=0.62.$$

From figure 25, curve *f*, $\delta=0.59$.

WALL EFFECT

It was pointed out earlier that the term δ, the fractional voids, accounts for the wall effect. That this is correct is shown by figure 25, as follows: It is known that the loosest packing of uniform spheres is the cubical arrangement ($\delta=0.4764$); however, δ in figure 25 is larger than 0.4764 for values of D_p/D_t larger than 0.34. The reason for this is that the wall effect causes the packing density near the container wall to be smaller than that found in the center of the tube.

LIMITS OF VOID FUNCTION

Comparison of various pressure-drop correlations indicates that a general agreement exists as far as effect of most variables upon pressure drop is concerned. However, agreement concerning the influence of the effect of the voids, the most significant variable, upon the pressure drop is least apparent. For comparison, the void functions used by a few investigators are listed in table 7.

According to publications listed in footnotes 16, 20, 30, 34, 36, 37, 38, 39, on pages 4 to 6 the pressure drop approaches infinity in beds of $\delta=0$. This would indicate that a bed of zero voidage is impermeable to fluid flow. Publications in footnotes 24, 30, 34, 36, and 37 on pages 5 and 6, on the other hand, suggest zero pressure drop for $\delta=1.0$. As this is not possible, it appears that pressure drop through packed columns should be considered as the sum of the pressure drop through the packing and the pressure drop caused by the pipe wall. In actual practice, however, the component of the pressure drop caused by the pipe wall is so small that it may generally be disregarded. Several other correlations suggest that unity pressure drop results for $\delta=1.0$, a result not readily conceivable. The correlation advanced by Brownell and Katz [30] has been developed in such a manner that at the condition $\delta=1.0$ the pressure drop is reduced to that of the empty pipe; Lapple [31] has expressed some doubt as to the continuity of their function chosen, and especially extension to high values of porosity.

[30] Work cited in footnote 39, p. 6.

[31] Lapple, C. E., Discussion of paper "Flow of Fluids Through Porous Media. I": Chem. Eng. Progress, vol. 43, 1947, pp. 537–548.

TABLE 7.—*Voidage functions of various investigators*

Literature survey ref. No.	Void function	Value of void function		Authors
		$\delta=0$	$\delta=1$	
20	$\delta^{-4/3}$	∞	1	Bakhmeteff and Feodoroff.
30	$\frac{(1-\delta)^{1.2}}{\delta^3}$	∞	0	Blake.
39	δ^{-n}	∞	1	Brownell and Katz.
34	$\frac{(1-\delta)^{3-n}}{\delta^3}$	∞	0	Burke and Plummer.
36	$\frac{(1-\delta)^{1.1}}{\delta^3}$	∞	0	Carman.
16	δ^{-2}	∞	1	Chalmers et al.
5	δ	0	1	Dupuit.
24	$(1-\delta)^3$	1	0	Happel.
37	$\frac{(1-\delta)^{3-n}}{\delta^3}$	∞	0	Hatch.
21	δ^2	0	1	Hatfield.
38	$\delta^{-1.7}$	∞	1	Oman and Watson.

The work of Happel [32] represents a comprehensive study of the variables involved in the pressure drop encountered in moving beds of the type used in Thermofor catalytic cracking units as well as in pebble heaters and similar equipment. His void function reduces to the finite value of 1.0 for $\delta=0$, a result that is not readily visualized from experience. Nevertheless, Happel achieved a very good correlation of his data despite the fact that the expression does not include a shape factor. Voidages in the various beds ranged between 32.7 and 49.2 percent and were chiefly the result of using various shapes of particles, rather than compacting beds of the same particles. For this reason, it seems doubtful whether the results of Happel will be applicable to beds of substantially different voidage than that stated above.

SADDLES

No attempt has been made to correlate voidages in beds composed of saddles and various types of special rings. The percentage voids for Berl saddles is higher than for most con-

[32] Work cited in footnote 24, p. 5.

ventional packing materials; consequently, the wall effect should be less pronounced for a packed column made up of Berl saddles than for a column consisting of other particles. For this reason, voids in such beds may be estimated satisfactorily from manufacturer's data.

SAMPLE CALCULATION

Brass rings have been dumped into a 1-inch standard pipe, and air is passed through the apparatus. Find the pressure drop across the unit for the following operating conditions:

Brass rings:

O. D. = 0.375 in.

I. D. = 0.250 in.

Height = 0.375 in.

Vessel:

$D_t = 0.0872$ ft.

Packing height, L = 0.873 ft.

Air:

Temperature = 75° F.

Inlet pressure = 15.5 p.s.i.a.

Rate = 48.8 lb./hr.

Calculations:

Ring volume $= (0.375^2 - 0.250^2)(0.785)(0.375) = 0.0227$ in.^{3}

Diameter of equivalent volume sphere =

$$D_p = \sqrt[3]{\frac{(0.0227)(6)}{\pi}} = 0.350 \text{ in.}$$

Voids:

First find the voids for a solid cylinder of diameter = 0.375 in. and height = 0.375 in.

Cylinder volume $= (0.375)^2\ (0.785)\ (0.375) = 0.0411$ in.^{3}
Diameter of equivalent volume sphere =

$$D_p = \sqrt[3]{\frac{(0.0411)(6)}{\pi}} = 0.430 \text{ in.};$$

$$\frac{D_p}{D_t} = \frac{0.430}{1.049} = 0.410;$$

from curve d of figure 25, $\delta = 0.50$;

volume of packed column $= (1.049)^2\ (0.785)\ (10.5) = 9.04$ in.^{3}

solid volume of cylinders in packed column $= (9.04)(1.00 - 0.50) = 4.52$ in.^{3}

number of cylinders in packed column $= \frac{4.52}{0.0411} = 110.$

Assuming that a column packed with brass rings also contains 110 pieces, the

solid volume of rings $= (110)\ (0.0227) = 2.50$ in.^{3}

δ for bed packed with rings $= \frac{9.04 - 2.50}{9.04} = 0.724.$

$$\frac{1-\delta}{\delta^3} = \frac{1-0.724}{0.724^3} = 0.732.$$

Modified Reynolds number:

$$G = \frac{(48.8)(144)}{(1.049)^2(0.785)} = 8{,}150 \text{ lb. hr.}^{-1} \text{ ft.}^{-2}$$

$$Re = \frac{(8150)(0.350)}{(12)(0.018)(2.42)} = 5{,}450.$$

From figure 25, $f = 0.725$ (curve for smooth particles).

Shape factor:

From page 16, $\lambda = 0.205\ \frac{A}{V_p^{2/3}}$.

For the brass rings:

$$\lambda = 0.205\ \frac{0.857}{(0.0227)^{2/3}} = 2.20,$$

$$\lambda^{1.1} = 2.38.$$

Density:

As the pressure drop will be small, calculate ρ on the basis of the inlet pressure.

$$\rho = \frac{(29)(492)(15.5)}{(359)(535)(14.7)} = 0.0784 \text{ lb./ft.}^3$$

Pressure drop

$$\Delta p = \frac{(0.0139)(0.725)((8.15)^2(10)^6(2.38)(0.732)(12)}{(0.350)(0.0784)(4.18)(108)} =$$

1.21 p. s. i./ft.

COMPARISON BETWEEN TOWER PACKINGS

BED-CHARACTERIZATION FACTOR

From a design point of view it is desirable to have a method for comparing characteristics of various packings without resorting to experimental work. With the introduction of a few simplifications, equation (14) may be used for such an analysis.

As the shape factor of particles likely to be used with equation (14) ranges between 1 (for spheres) and 3 (for some saddles), a maximum error of only 6 percent is introduced into the equation by modifying it to read:

$$\Delta P = \frac{2.12 f G^2 L \lambda (1-\delta)}{D_p g_c \rho \delta^3}. \qquad (21)$$

Figure 10 shows that, for the turbulent range covered by equation (21), moderate variations in Reynolds numbers affect the magnitude of f only insignificantly. Equation (21) may therefore be written in the form:

$$\Delta P \cong c\ \frac{G^2}{\rho}\ \frac{L\lambda(1-\delta)}{D_p \delta^3}\ , \qquad (22)$$

where c is an experimental constant.

Designating $\frac{G^2}{\rho}$ by ϕ' and $\frac{L\lambda(1-\delta)}{D_p\,\delta^3}$ by β, one may write:

$$\Delta P \propto \phi'\beta. \qquad (22a)$$

As β is a function of the packing material and the apparatus dimensions only and had no effect upon the flow factor, ϕ', it has been termed the bed-characterization factor. The new concept is especially convenient as a criterion for tower-packing performance. It is desirable in this connection to let L=unity, because it enters the pressure-drop equation as a multiplier only. The bed-characterization factor will be used to compare Raschig rings, Berl saddles, and Lessing rings. Table 8 lists characteristics of the packing elements as reported by the manufacturer (Knight-Ware).

TABLE 8.—*Packing characteristics of Raschig rings, Berl saddles, and Lessing rings, as reported by the manufacturer*

Packing [1]	Number of pieces per ft.³, dumped	Fractional voids (δ)	Surface area, ft.²/ft.³
Raschig rings:			
¼	88, 000	0. 52	220
½	10, 700	. 53	114
1	1, 330	. 68	58
1½	380	. 68	36
Berl saddles:			
¼	113, 000	. 58	274
½	17, 600	. 60	155
1	2, 300	. 69	79
1½	690	. 70	52
Lessing rings:			
1	1, 300	. 66	69
1¼	650	. 62	53
1½	350	. 60	40
2	150	. 68	32

[1] Nominal size, inches.

Assuming a cylindrical vessel 12 inches in diameter and 12 inches high, then for 1-inch Raschig rings:

$$N=(1{,}330)(0.785)=1{,}042$$

$$A=\frac{(0.58)(144)}{1{,}330}=6.29 \text{ in.}^2$$

$$V_p=\frac{(0.32)(1{,}728)}{1{,}330}=0.415 \text{ in.}^3$$

$$D_p=\sqrt[3]{\frac{(0.415)(6)}{\pi}}=0.925 \text{ in.}$$

$$\lambda=(0.205)\ \frac{0.29}{(0.415)^{2/3}}=2.32$$

$$\beta=\frac{(2.32)(0.32)}{(0.925)(0.313)}=2.56$$

$$V_P=(1{,}042)(0.415)=433 \text{ in.}^3$$

$$A_P=(1{,}042)(6.29)=6{,}570 \text{ in.}^3$$

The above data for rings may also be approximated by starting from solid cylinders 1 inch in diameter and 1 inch high. For the cylinder,

$$D_p=1.148,$$

and

$$\frac{D_p}{D_t}=\frac{1.148}{12}=0.0957.$$

From curve "e" of figure 25,

$$\delta=0.365.$$

Then,

$$N=\frac{(0.635)(0.785)(1{,}728)}{0.785}=1{,}100.$$

For a standard Raschig ring $d_o=h=1$ inch and $d_i=0.75$ inch, $V_p=(1)(1-0.56)=0.44$ inch.³ Assuming 1,100 rings in the vessel,

$$\delta=\frac{(1{,}728)(0.785)-(1{,}100)(0.44)}{(1{,}728)(0.785)}=0.645.$$

$$A=6.188 \text{ in.}^2$$

$$D_p=0.945 \text{ in.}$$

$$\lambda=2.19;\ \beta=3.08,$$

$$V_P=484;\ A_P=6{,}800.$$

For 1-inch Berl saddles:

$$N=(2{,}300)(0.785)=1{,}810$$

$$A=\frac{(79)(144)}{2{,}300}=4.95 \text{ in.}^2$$

$$V_p=\frac{(0.31)(1{,}728)}{2{,}300}=0.233 \text{ in.}^3$$

$$D_p=\sqrt[3]{\frac{(0.233)(6)}{\pi}}=0.765 \text{ in.}$$

$$\lambda=\frac{(0.205)(4.95)}{(0.233)^{2/3}}=2.68$$

$$\beta=\frac{(0.31)(2.68)}{(0.69)^3(0.765)}=3.31$$

$$V_P=(1{,}810)(0.233)=421 \text{ in.}^3$$

$$A_P=(1{,}810)(4.95)=8{,}770 \text{ in.}^2$$

The calculations for the other packings were made in the same manner. A summary of the calculated results appears in table 9.

TABLE 9.—*Particle and bed characteristics for towers, packed Raschig rings, Berl saddles, and Lessing rings*

(TURBULENT FLOW)

Nominal size, inches	N	A, sq. in.	V_p, cu. in.	D_p, in.	λ	δ	β	A_P, sq. in.	V_P, cu. in.	A_c, sq. in.	V_c, cu. in.
Raschig rings:											
¼	69, 000	0. 360	0. 0094	0. 236	1. 65	0. 52	24. 0	24, 900	652	1, 040	27. 2
½	8, 400	1. 535	. 0756	. 526	1. 75	. 53	10. 6	12, 930	636	1, 200	60. 0
1	1, 042	6. 29	. 415	. 925	2. 32	. 68	2. 56	6, 570	433	2, 560	170
1¼	1, 100	6. 19	. 440	. 944	2. 19	. 65	3. 10	6, 800	484	2, 190	156
1½	299	13. 65	1. 455	1. 405	2. 19	. 68	1. 60	4, 070	432	2, 540	270
Berl saddles:											
¼	88, 500	. 350	. 0064	. 231	2. 07	. 58	20. 4	31, 100	570	1, 530	27. 8
½	13, 800	1. 27	. 0393	. 422	2. 24	. 60	9. 9	17, 600	544	1, 790	55. 0
1	1, 810	4. 95	. 233	. 765	2. 68	. 69	3. 31	8, 770	421	2, 650	128
1½	542	10. 9	. 750	1. 13	2. 71	. 70	2. 11	5, 910	406	2, 810	193
Lessing rings:											
1	1, 020	7. 64	. 452	. 953	2. 67	. 66	3. 31	7, 790	461	2, 350	139
1¼	510	11. 77	1. 008	1. 243	2. 43	. 62	3. 10	6, 000	514	1, 930	166
1½	350	16. 5	1. 975	1. 558	2. 17	. 60	2. 57	4, 545	544	1, 770	212
2	150	30. 7	3. 69	1. 921	2. 67	. 68	1. 40	3, 625	435	2, 590	311

[1] Voidage date estimated from cylinders, using fig. 25.

VOLUME AND SURFACE-AREA CHARACTERISTICS

Table 9 introduces two new concepts—the volume characteristic, V_c, and the surface area characteristic, A_c, of a packing. By definition:

$$V_c=\frac{V_P}{\beta}. \tag{23}$$

$$A_c=\frac{A_P}{\beta}. \tag{24}$$

These concepts are more significant than β alone for comparing tower packings with each other. Depending on whether the surface area or the solid volume is of importance in the operation, the comparison should be made on the basis of A_c or V_c, respectively.

Results in the table show that, for comparable sizes, the Berl saddles have higher values of A_c than either Raschig or Lessing rings. This indicates that for the three packings considered the saddles offer the least pressure drop for a given surface area. On the other hand, comparison of V_c values indicates that the saddles will provide the least mass inside the tower for a comparable pressure drop. These properties are chiefly responsible for the comparatively wide distribution of Berl saddles in distillation, absorption, and stripping equipment.

From the operation of packed towers and reactors, it is known that the entire charge of the vessel is not always effective in the desired operation. Frequently, because of faulty charging of the vessels, bridging of the packing elements occurs, and the fluids, using the path of least flow resistance, bypass the denser portions of the bed. This phenomenon is related to channeling and will be discussed in greater detail in connection with fluidization. While this cause of inefficiency may be largely overcome by loading the vessel carefully, there are other more inherent reasons why certain portions of packed beds are less effective than others. Thus, it is conceivable that with certain types of rings of very small internal diameter, the inside area is less effective in an operation because of the comparative ease of blocking. Taking this into consideration, it appears that true characteristic volumes and surfaces should be defined by

$$V_c=\frac{V_P}{\beta}k_v \tag{25}$$

and

$$A_c=\frac{A_P}{\beta}k_a, \tag{26}$$

where k_v and k_a are constants pertaining to the individual packing elements and denoting the fraction of the packing that is effective. The constants are dependent on bed configuration and can only be determined experimentally. Pressure-drop observations through conventional Raschig rings have indicated that the ring interior is apparently no less effective than the inter-particle voids, and therefore, for rings, one may assume that $k_a=k_v=1$. For more complex packings, such as certain types of partition rings, the constants are probably considerably smaller than unity.

RELATIVE PACKING EFFICIENCY

Comparison of A_c and V_c values of one packing with those of another suggests the

introduction of a term for relative packing efficiency. Thus, with reference to surface area:

$$E_{ra}=\frac{(A_c k_a)_x}{(A_c k_a)_y}, \tag{27}$$

$$E_{rv}=\frac{(V_c k_v)_x}{(V_c k_v)_y}, \tag{28}$$

where subscripts x and y refer to the less efficient and more efficient packing, respectively.

SPACE VELOCITY

It has become customary in catalytic process development to describe the feed rate of fluid (gas, vapor, or liquid) into a reactor in terms of space velocity. In English units, space velocity is defined as the number of cubic feet of the feed per cubic foot of catalyst per hour. The term "cubic foot of catalyst" refers to 1 cubic foot of reactor volume "filled with catalyst," not taking into account packing density. The concept may be expressed by the simple equation:

$$\bar{S}=\frac{G}{L\rho}. \tag{29}$$

An improved definition, which compensates for packing density, is given by:

$$S=\frac{G}{L\rho(1-\delta)}. \tag{30}$$

Depending on whether the reaction proceeds chiefly on the outside surface or in the interior of the catalyst, a somewhat more exact definition of space velocity is possible:

$$S=\frac{G}{L\rho(1-\delta)k_a} \tag{31}$$

for surface reactions and

$$S=\frac{G}{L\rho(1-\delta)k_v} \tag{32}$$

for reactions proceeding in the catalyst interior. Because k_a and k_v are close to unity for carefully packed reactors, equations (31) and (32) reduce to the form of equation (30). The following calculation will show the magnitude of error that may be involved in the design of reactors if the definition of space velocity as given by equation (29) is used.

A Fischer-Tropsch catalyst was reduced by means of hydrogen at 450° C. A 0.375-inch standard pipe packed to a depth of 10 inches with alundumlike cylindrical pellets ($h=d=$ 0.125 inch) was used as a reactor, and the inlet gas rate was 1.100 standard ft.^{3}/hr. A larger unit, using 110 ft.^{3}/hr. of hydrogen, is to be installed, and it has been decided to use a 2-inch standard pipe as reactor. To what depth will the unit have to be charged with catalyst of the same size if the operation is to proceed at the same space velocity that was employed in the exploratory unit?

SOLUTION

Hydrogen density:

$$\rho=\frac{(2)\,(492)}{(359)\,(530)}=0.0052 \text{ lb./ft.}^3$$

Reactor cross-sectional area: 0.001326 ft.^{2}
Mass velocity:

$$G=\frac{(1.10)\,(0.0052)}{0.001326}=4.31 \text{ lb. hr.}^{-1} \text{ ft.}^{-2}$$

Space velocity:

$$\bar{S}=\frac{(4.31)\,(12)}{(10)\,(0.0052)}=1{,}000.$$

Mass velocity in large unit:

$$G=\frac{(110)\,(0.0052)}{0.0233}=24.5 \text{ lb. hr.}^{-1} \text{ ft.}^{-2}.$$

According to equation (29),

$$L=\frac{24.5}{(1{,}000)\,(0.0052)}=4.72 \text{ ft.}$$

In order to use equation (30), the respective bed voidages must be found first.

From figure 26, $\lambda=1.145$ for the cylinders under consideration. The effective particle diameter:

$$D_p=\frac{3\lambda}{\left(\frac{1}{h}+\frac{2}{d_c}\right)}=\frac{(3)\,(1.145)}{(8+16)}=0.143 \text{ in.}$$

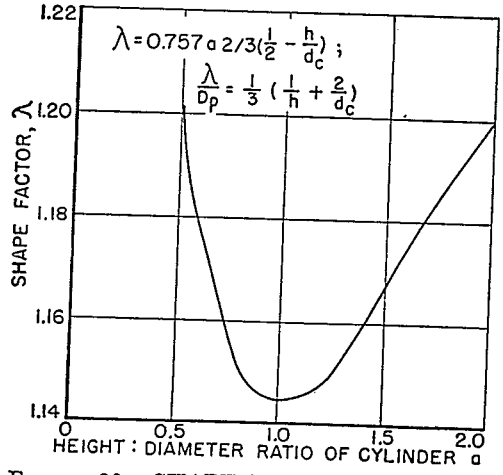

FIGURE 26.—SHAPE FACTOR IN RELATION TO HEIGHT: DIAMETER RATIO FOR CYLINDRICAL BODIES.

For the exploratory unit,

$$\frac{D_p}{D_t}=\frac{0.143}{0.493}=0.29,$$

and from figure 25, curve e, $\delta=0.482$. For the large tube,

$$\frac{D_p}{D_t}=\frac{0.143}{2.067}=0.069,$$

and $\delta=0.355$.

Using equation (30), the true space velocity

$$S=\frac{(4.31)\,(12)}{(10)\,(0.0052)\,(1-0.482)}=1{,}920,$$

and again using the equation,

$$L=\frac{24.5}{(1{,}920)\,(0.0052)\,(1-0.355)}=3.82 \text{ ft.}$$

The error introduced into the calculations by using equation (29) amounts to

$$\frac{(4.72-3.82)\,(100)}{3.82}=23.6 \text{ percent.}$$

This error may become substantially larger for different packing materials and greater scale-up ratios.

CYLINDERS, SPHERES, AND GRANULES

The catalyst shapes most frequently used in industrial work are cylinders, spheres, and granules. Although, as will be seen later, these shapes do not offer such favorable conditions as do rings or Berl saddles, the cost of their preparation is smaller, and they exhibit considerably greater mechanical strength.

CYLINDERS

Calculation of λ and $\frac{\lambda}{D_p}$ ratio.

Consider a solid cylinder of length h, diameter $d_c=2_{\gamma pc}$, and $h/d_c=a$. Then,

$$\frac{\lambda}{D_p}=\frac{A_p}{6V_p}=\frac{\left[\frac{2\pi d_c^2}{4}+\pi d_c h\right]}{\frac{6\pi d_c^2 h}{4}},$$

$$\frac{\lambda}{D_p}=\frac{\frac{\pi d_c}{2}(d_c+2h)}{\frac{3\pi d_c}{2}(d_c h)}=\frac{d_c+2h}{3d_c h}=\frac{1}{3}\left[\frac{1}{h}+\frac{2}{d_c}\right]. \quad (33)$$

Also,

$$\lambda=0.205\,\frac{A_p}{V_p^{2/3}}=\frac{0.205\left[\frac{2\pi d_c}{4}+d_c h\right]}{\left[\frac{\pi d_c^2}{4}h\right]^{2/3}};$$

which reduces to:

$$\lambda=0.757\,a^{2/3}\left[\frac{1}{2}+\frac{1}{a}\right]. \quad (33a)$$

In figure 26, shape factors for cylinders have been plotted in relation to the height/diameter ratio. It is observed that the curve passes through a minimum at $a=1$, a condition that is easily predicted by the conventional methods of calculus.

Because the height and the diameter are known for most cylindrical pellets, the curve in figure 26, in combination with equation (33), offers a rapid method of arriving at the equivalent particle diameter.

Tables 10, 11, and 12 list the calculated data pertaining to beds of cylinders, spheres, and granules. In all three cases the vessel chosen was 3 inches I. D. and was packed to a depth of 1 foot in such a manner that the voidages reported in figure 25 applied to the systems. The surface of the materials was assumed to be smooth.

TABLE 10.—*Calculated data for cylinders*

Dimensions, inches	D_p, inch	D_p/D_t	δ	N	A, sq. in.	V_p, cu. in.	β	A_P, sq. in.	V_P, cu. in.	$\frac{A_P}{\beta}=A_c$, sq. in.	$\frac{V_P}{\beta}=V_c$, cu. in.
1/16×1/16	0.0715	0.0238	0.320	301,000	0.01842	0.0001918	3,980	5,550	57.3	1.396	0.0145
1/8×1/8	.143	.0477	.330	37,050	.0737	.001532	1,786	2,735	56.8	1.530	.0318
1/4×1/4	.286	.0953	.340	4,560	.2946	.01226	810	1,348	55.9	1.664	.0692
3/8×3/8	.429	.143	.360	1,312	.633	.0414	439	830	54.3	1.888	.1240
7/16×7/16	.5005	.1668	.368	814	.903	.0659	349	734	53.5	2.100	.1537
1/2×1/2	.572	.1907	.377	538	1.178	.09813	282	634	52.9	2.25	.1875
5/8×5/8	.715	.2383	.400	265	1.842	.1917	182.5	48.8	50.8	2.68	.2785
3/4×3/4	.858	.286	.429	146	2.643	.331	116.5	386	48.3	3.32	.4148

TABLE 11.—*Calculated data for spheres*

D_p, inches	D_p/D_t	δ	N	A, sq. in.	V_p, cu. in.	β	A_P, sq. in.	V_P, cu. in.	$\frac{A_P}{\beta}=A_c$, sq. in.	$\frac{V_P}{\beta}=V_c$, cu. in.
0.150	0.05	0.345	31,450	0.0706	0.00177	1,288	2.222	55.7	1.728	0.0433
.30	.10	.368	3.802	.2826	.01412	508	1,076	53.8	2.12	.1060
.525	.175	.400	671	.864	.0758	214	579	50.9	2.70	.238
.81	.270	.442	170	2.07	.2775	96	352	47.3	3.67	.493
1.02	.340	.473	81	3.26	.5545	58.8	264	44.9	4.49	.762
1.26	.420	.522	42	5.00	1.048	31.9	210	43.9	6.58	1.380
1.44	.480	.538	25	6.50	1.57	24.6	162.5	39.3	6.60	1.59

TABLE 12.—*Calculated data for magnetite granules*

D_p, inches	D_p/D_t	δ	N	A, sq. in.	V_p, cu. in.	β	A_P, sq. in.	V_P, cu. in.	$\frac{A_P}{\beta}=A_c$, sq. in.	$\frac{V_P}{\beta}=V_c$, cu. in.
0.15	0.05	0.443	26,675	0.1223	0.00177	888	3,268	47.3	3.68	0.0533
.30	.10	.477	3.135	.4898	.01412	334	1,537	44.2	4.60	.1328
.525	.175	.491	570	1.495	.0758	170	853	43.3	5.01	.254
.81	.270	.508	150	3.58	.2775	96.6	537	41.6	5.55	.430
1.02	.340	.517	74	5.64	.5545	71.5	417	41.0	5.82	.572

Significant data for the three packings are shown graphically in figures 27 and 28. From figure 27 relating total bed surfaces and volumes to the ratio of packing to vessel diameter, it appears that the bed composed of granules has the greatest surface. The cylindrical bed has a somewhat smaller surface, and the spheres exhibit the least surface of all the materials.

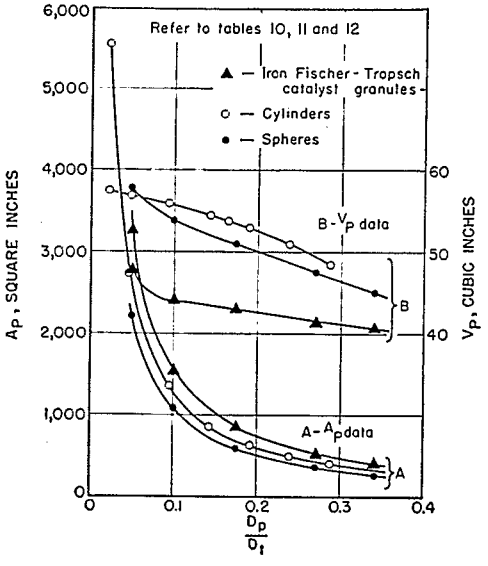

FIGURE 27.—SURFACE AREAS AND SOLID VOLUMES FOR VARIOUS TOWER PACKINGS IN PIPE OF D_t=3 INCHES.

This is directly related to the particle shape factor of the materials; that is, granules, λ=1.73; cylinders, λ=1.145; and spheres, λ=1.00. As far as volume of packing material is concerned, the cylinders are most effective, spheres are

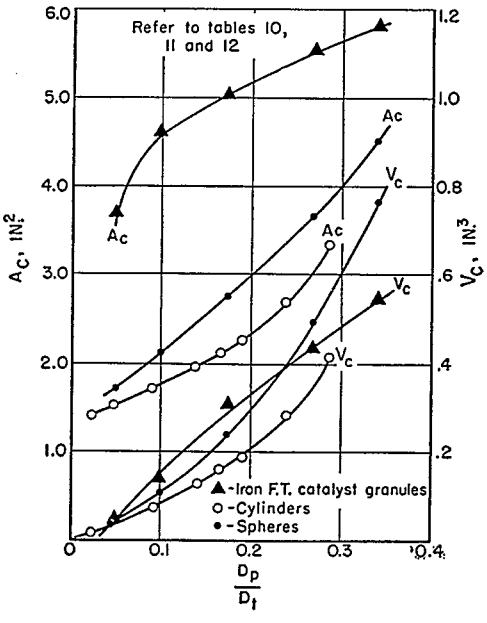

FIGURE 28.—VOLUME AND AREA CHARACTERISTICS FOR VARIOUS TOWER PACKINGS SUBJECT TO TURBULENT FLOW.

second most effective, and the granules produce a bed of least density. This characteristic is in line with the voidages of the individual beds. Figure 25 indicates that the granular beds have a considerably higher voidage than either spheres or cylinders.

Comparison of characteristic areas and volumes should be very significant. In figure 28, values of A_c and V_c have been shown for packing materials in their relation to the particle/tube-diameter ratio. The positive slope of all the curves indicates that both A_c and V_c values increase with increasing D_p/D_t ratio. As far as V_c is concerned, the three packings do not differ much from each other. With respect to A_c, however, it appears that the granules are, by far, the most efficient packing. To decide which material is best suited for a specific purpose, values of A_P, V_P, A_c, and V_c must be considered together in their relation to the process. From the analysis presented, it appears that the granules are preferable to both spheres or cylinders.

Values of A_c and V_c in tables 10, 11, and 12 may readily be compared with those in table 9 after the latter have been divided by

$$\left(\frac{12}{3}\right)^2=16$$

(because the data in the latter table are based on a 12-inch diameter vessel). Such a comparison indicates that rings and saddles are better than cylinders, spheres, or granules in every respect. Their use in catalysis, however, is curtailed because of the comparatively high cost of their production. Furthermore, these packings have less mechanical strength than cylinders, spheres, or granules, another major factor to be considered in the choice of a packing.

SUMMARY

From an analogy of flow through empty pipes, an equation was derived applying to flow through packed tubes. After evaluation of the experimental constants, the equation had the form:

$$\Delta P=\frac{2.12fG^2\lambda L(1-\delta)}{D_p g_c \rho \delta^3}, \qquad (21)$$

and the influence of each variable upon the pressure drop was experimentally established. For smooth particles such as glass or porcelain, the modified friction factor, f, was given by the relation:

$$f=1.75\left(\frac{D_pG}{\mu}\right)^{-0.1}. \qquad (13)$$

With rougher materials such as alundum or clay, the friction factor,

$$f=2.625\left(\frac{D_pG}{\mu}\right)^{-0.1}. \qquad (16)$$

For still rougher particles, for example, Aloxite or MgO granules,

$$f=4.00\left(\frac{D_pG}{\mu}\right)^{-0.1}. \qquad (17)$$

Thus, by selecting the proper friction factor for each material, the validity of the equation has been extended to materials of different degrees of surface roughness. An absolute measure of roughness has been proposed by expressing the property by the ratio e/r_p, where e is the height of the protuberances on the particle surface, and r_p is the effective particle diameter. As roughness specifications are not available from manufacturers' data, however, a correlation between f and e/r_p was not possible, and the problem could only be dealt with descriptively.

One of the major factors in detecting the effect of roughness was an understanding of the effect of the voids upon the pressure drop. Experimental data revealed that a small variation in voids, for example, 40 to 43 percent, influences the pressure drop by as much as 23 percent. The range of voids (35 to 76 percent) pertaining to the experimental data upon which the equations are based was covered by the function

$$\frac{(1-\delta)}{\delta^3}$$

with very good results. Despite the variation of D_p/D_t (from 0.047 for MgO granules to 0.615 for porcelain balls), no wall-effect factor is required to use the equation. It is believed that wall effect is accounted for if the total voids are substituted into the equation. The equation contains a shape factor that accounts for the effect of packing surface upon the pressure drop. By derivation, shape factor

$$\lambda=0.205\frac{A}{V_p^{2/3}}. \qquad (9)$$

The usefulness of the concept became apparent through the application of the equation to beds of spheres, cylinders, rings, Berl saddles, and granules. Without the shape factor in the equation, predicted values of pressure drop for differently shaped particles would vary by several hundred percent.

A separate study was undertaken to develop a correlation of voids in packed tubes. A simple correlation between δ and D_p/D_t was found possible for the various shapes investigated. This development is important, because, without the knowledge of the void content of a packed bed, the usefulness of any pressure-drop correlation would be greatly hampered; this correlation has many other applications, also. For instance, it facilitates prediction of vessel capacities for specific packings and estimation of surface areas in packed towers.

Finally, an analysis of the equation showed that it may be used directly to predict the individual merits of tower packings. In this connection, a new concept, the bed-characterization factor, was introduced. In combination with surface area and volume of the packing, bed-characterization factors were found important as a criterion for comparison of tower packings.

PRESSURE DROP THROUGH PACKED TUBES, VISCOUS FLOW

GENERAL CORRELATION

In the previous section, it has been demonstrated that equation (5)

$$\Delta p=\frac{k}{g_c}\left(\frac{D_p G}{\mu}\right)^n\left(\frac{\mu^2}{\rho}\right)\left(\frac{\lambda^{3-n}}{D_p{}^3}\right)\frac{(1-\delta)^{3-n}}{\delta^3}$$

applies to turbulent flow through packed tubes as n approaches 2. However, the equation also covers the viscous flow range if a value of $n=1$ is used. With this substitution, (5) becomes:

$$\Delta p=\frac{k}{g_c}\frac{D_p G}{\mu}\frac{\mu^2}{\rho}\frac{\lambda^2}{D_p{}^3}\frac{(1-\delta)^2}{\delta^3}, \tag{34}$$

or:

$$\Delta p=\frac{kG\mu\lambda^2(1-\delta)^2}{D_p{}^2 g_c\rho\delta^3}. \tag{35}$$

In (35), Δp has the dimension pounds per square foot per foot. Later extension of the equation to fluidization will show that it is more convenient to use the form

$$\Delta P=\frac{kGL\mu\lambda^2(1-\delta)^2}{D_p{}^2 g_c\rho\delta^3}, \tag{36}$$

where ΔP now has the dimension pounds per square foot. Comparing ΔP in the form of equation (36) with a modified form of the Fanning equation,

$$\Delta P=\frac{2fG^2L(1-\delta)^2}{D_p\rho g_c\delta^3}, \tag{37}$$

which may be considered applicable to fluid flow through packed sections, it follows that

$$f=C\left(\frac{D_p G}{\mu}\right)^{-1}, \tag{38}$$

where C is a constant that must be evaluated experimentally. From equation (37) it also appears that

$$f=\frac{\Delta P D_p\rho g_c\delta^3}{2G^2L(1-\delta)^2}, \tag{37a}$$

which may be evaluated from experimental data.

Examination of (37) does not account for the shape of the particles. Therefore, equation (38) suggests that if log f-values are plotted versus the respective values of

$$\log\frac{D_p G}{\mu},$$

a series of straight lines of slope $n=-1$ should result. The displacement of the lines from each other should be a result of the effect of shape factor of the packing upon the pressure drop. From relation

$$\Delta p\propto\lambda^2 \tag{36a}$$

and this displacement, the shape factor of the various materials may be estimated.

DATA AND EQUIPMENT

Tables 13 to 19 present the keys to figures 29 to 34. The original data are given in tables

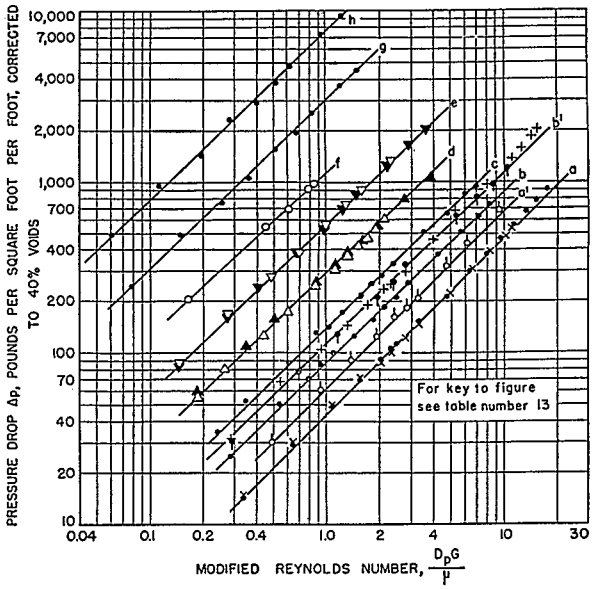

FIGURE 29.—DOWN FLOW OF GASES THROUGH SAND BEDS.

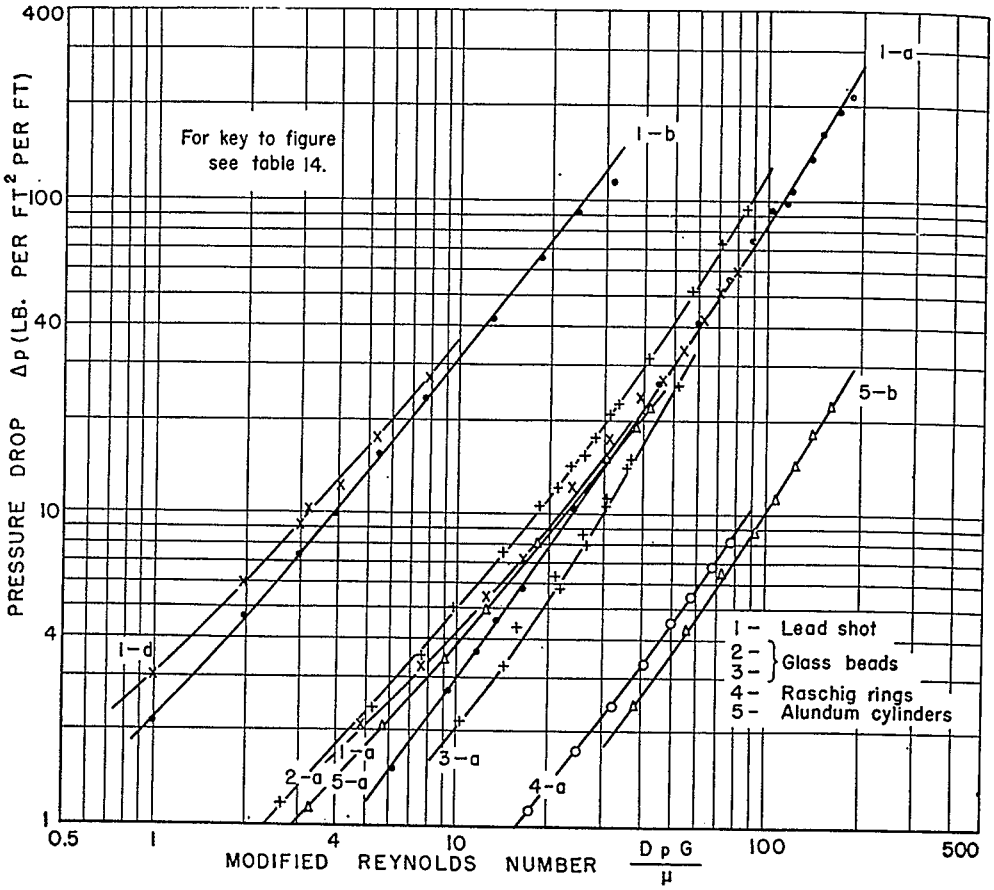

FIGURE 30.—DOWN FLOW OF GASES THROUGH VARIOUS MATERIALS.

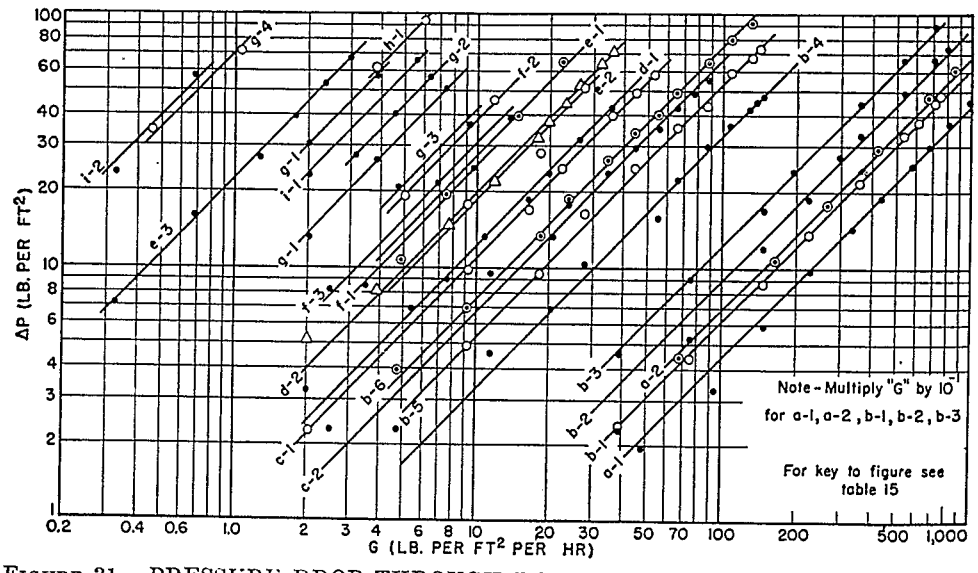

FIGURE 31.—PRESSURE DROP THROUGH ROUND SAND (COUNTER-GRAVITY FLOW) IN 2½-INCH TUBE.

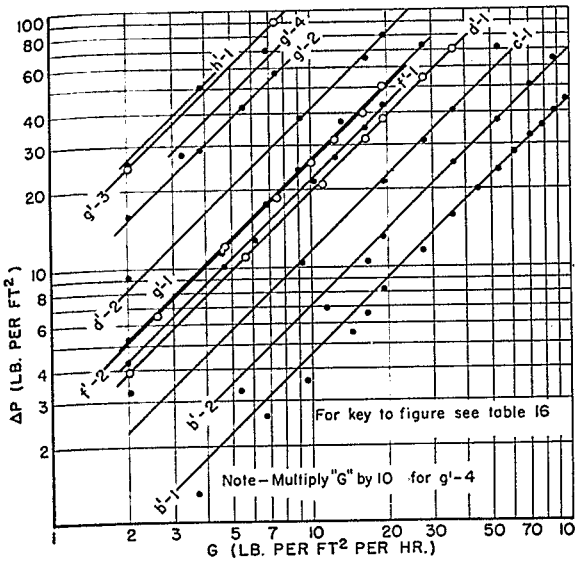

FIGURE 32.—PRESSURE DROP THROUGH SHARP SANDS IN 2½-INCH TUBE (COUNTER-GRAVITY FLOW).

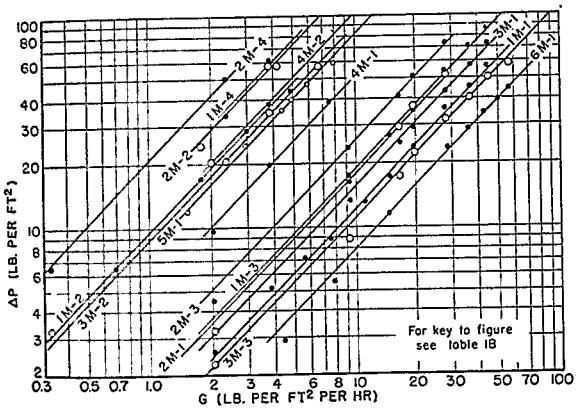

FIGURE 33.—PRESSURE DROP THROUGH ROUND AND SHARP SANDS IN 4-INCH TUBE (COUNTER-GRAVITY FLOW).

V and VI of the appendix. Figure 29 shows measurements made with sands under co-gravity flow conditions. The apparatus was a 1-inch standard pipe carrying a 200-mesh screen on the lower end. As the flow rates were small, the pressure drop across the screen could be neglected in all cases. Air and helium were used as fluids to investigate the effect of kinematic viscosity on the pressure drop. From the specific gravity of the sand (2.65), the

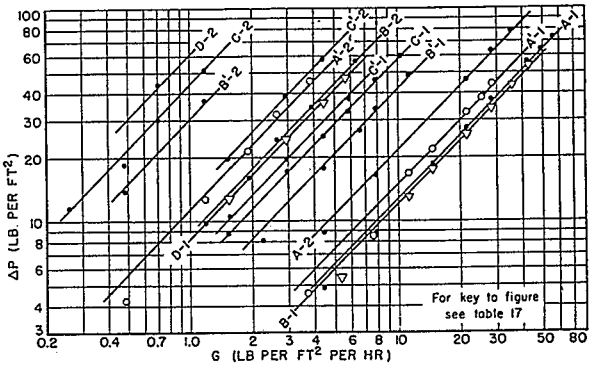

FIGURE 34.—PRESSURE DROP THROUGH MIXTURES OF SANDS (COUNTER-GRAVITY FLOW).

weight of the sand in the tube, and a knowledge of the height of the sand column, the fractional voids were calculated. The data reported in table 13 were collected with narrow cuts of sand. The diameter of such a cut was defined by $D_p=\sqrt{d_1 d_2}$, where d_1 and d_2 are adjacent sieve openings.

The data referred to in table 14 pertain to larger particles. Unlike the sands of table 13, the lead shot, glass beads, Raschig rings, and cylinders permitted direct calculation of shape factor, and voids were determined by immersion in water. The flow of the air and helium was downward.

TABLE 13.—*Experiments with round and sharp sands in 1-inch standard pipe*

Run	D_p, inch	Fractional voids δ
a	0. 01505	0. 410
	. 01505	. 354
b	. 01268	. 386
	. 01268	. 350
c	. 01062	. 414
	. 01062	. 358
d	. 00818	. 435
	. 00818	. 367
e	. 00632	. 446
	. 00632	. 381
f	. 00488	. 445
	. 00488	. 391
g	. 00345	. 450
h	. 00264	. 485
a′	. 01505	. 486
b′	. 01268	. 494
	. 01268	. 431

TABLE 14.—*Experiments with large particles in 1-inch standard pipe*

(DOWNFLOW OF AIR AND HELIUM)

Run	D_p, inch	Material	Shape factor, λ	Fractional bed voids, δ	Gas	Surface
1–a	0. 0779	Lead shot	1. 00	0. 354	Air	Smooth.
1–b	. 0779	do	1. 00	. 354	Helium	Do.
1–c	. 0779	do	1. 00	. 382	Air	Do.
1–d	. 0779	do	1. 00	. 382	Helium	Do.
2–a	. 143	Glass beads	1. 00	. 378	Air	Do.
3–a	. 172	do	1. 00	. 388	do	Do.
				. 405	do	Do.
4–a	. 252	Raschig rings	1. 50	. 391	do	Do.
5–a	. 182	Alundum cylinders	1. 15	. 566	Helium	Rough.
5–b	. 182	Alundum cylinders	1. 15	. 362	do	Do.
				. 362	Air	Do.

TABLE 15.—*Experiments with uniform round sands in 2½-inch tube*

Run	D_p, inch	Weight, gm.	Static height, ft.	Static fractional voids, δ	Gas	Fluidization pressure drop, lb./sq. ft.	
						Observed	Calculated
a–1	0. 01505	756	0. 505	0. 422	Air	48	49
a–2	. 01505	1, 193	. 784	. 416	do	76	77
b–1	. 01268	750	. 489	. 410	do	46	49
b–2	. 01268	1, 150	. 754	. 414	do	72	75
b–3	. 01268	1, 511	. 980	. 408	do	96	98
b–4	. 01268	750	. 489	. 410	CO_2	47	49
b–5	. 01268	1, 150	. 748	. 410	do	72	75
b–6	. 01268	1, 511	. 977	. 407	do	97	98
c–1	. 01062	874	. 584	. 423	Air	57	57
c–2	. 01062	874	. 584	. 423	CO_2	57	57
d–1	. 00818	650	. 449	. 444	Air	43	42
d–2	. 00818	1, 116	. 724	. 447	do	75	72
e–1	. 00632	980	. 679	. 445	do	64	64
e–2	. 00632	980	. 676	. 443	CO_2	64	64
e–3	. 00632	980	. 669	. 436	Helium	66	64
f–1	. 00488	557	. 394	. 454	Air	35	36
f–2	. 00488	858	. 597	. 445	do	56	56
f–3	. 00488	858	. 590	. 442	CO_2	55	56
g–1	. 00345	898	. 656	. 474	Air	57	58
g–2	. 00345	1, 080	. 771	. 461	do	69	70
g–3	. 00345	898	. 656	. 474	CO_2	58	58
g–4	. 00345	1, 080	. 771	. 461	Helium	71	70
h–1	. 00310	1, 865	1. 473	. 511	Air	111	121
h–2	. 00310	2, 376	1. 890	. 516	do	139	154
h–3	. 00310	2, 376	1. 890	. 516	Helium	144	154
i–1	. 00290	1, 185	. 920	. 508	Air	69	77
i–2	. 00290	1, 185	. 920	. 508	Helium	70	77
j–1	. 00202	920	. 793	. 550	Air	51	60
j–2	. 00202	1, 339	1. 108	. 533	do	74	90
j–3	. 00202	1, 339	1. 090	. 528	Helium	76	90

TABLE 16.—*Experiments with uniform sharp sands in 2½-inch tube*

Run	D_p, inch	Weight, grams	Static height, feet	Static fractional voids, δ	Gas	Fluidization pressure drop, lb./sq. ft.	
						Observed	Calculated
b′–1	0. 01268	755	0. 580	0. 500	Air	47	49
b′–2	. 01268	1, 255	. 945	. 490	do	81	82
c′–1	. 01021	1, 150	. 900	. 510	do	70	75
d′–1	. 00818	1, 181	. 982	. 539	do	70	77
d′–2	. 00818	2, 181	1. 747	. 520	do	131	142
f′–1	. 00488	850	. 742	. 559	do	47	55
f′–2	. 00488	1, 150	1. 000	. 559	do	64	75
g′–1	. 00345	630	. 570	. 572	do	33	41
g′–2	. 00345	981	. 868	. 566	do	56	64
g′–3	. 00345	1, 759	1. 578	. 570	do	101	114
g′–4	. 00345	1, 759	1. 578	. 570	Helium	101	114
h′–1	. 00229	900	. 820	. 578	Air	50	58

TABLE 17.—*Experiments with uniform round and sharp sands in 4-inch tube*

Run	D_p, inch	Weight, grams	Static height, feet	Static fractional voids, δ	Gas	Fluidization pressure drop, lb./sq. ft.	
						Observed	Calculated
				Round sands			
A–1	0. 01100	3, 239	0. 891	0. 447	Air	80	82
A–2	. 01100	5, 508	1. 554	. 458	do	140	140
B–1	. 01062	2, 487	. 690	. 453	do	62	63
B–2	. 01062	2, 487	. 698	. 457	Helium	61	63
C–1	. 00445	2, 545	. 737	. 475	Air	63	64
C–2	. 00445	2, 545	. 737	. 475	Helium	63	64
D–1	. 00310	2, 355	. 786	. 545	Air	57	60
D–2	. 00310	2, 355	. 775	. 538	Helium	58	60
				Sharp sands			
A′–1	. 00715	2, 168	. 734	0. 550	Air	53	55
A′–2	. 00715	2, 168	. 727	. 548	Helium	53	55
B′–1	. 00458	2, 352	. 839	. 574	Air	57	60
B′–2	. 00458	2, 352	. 842	. 573	Helium	57	60
C′–1	. 00303	1, 793	. 658	. 587	Air	44	45
C′–2	. 00303	3, 541	1. 288	. 578	do	86	90

TABLE 18.—*Experiments with mixed round and sharp sands in 2½-inch and 4-inch tubes*

Run	D_p, inch	Weight, grams	Static height, feet	Static fractional voids, δ	Gas	Fluidization pressure drop, lb./sq. ft.	
						Observed	Calculated
			2½-inch tube				
1M-1	0. 0094	1, 000	0. 681	0. 437	Air	57	65
1M-2	. 0094	1, 000	. 681	. 437	Helium	58	65
1M-3	. 0094	1, 492	. 989	. 423	Air	87	97
1M-4	. 0094	1, 492	. 989	. 423	Heluim	87	97
2M-1	. 00838	1, 000	. 675	. 431	Air	58	65
2M-2	. 00838	1, 000	. 675	. 431	Helium	58	65
2M-3	. 00838	1, 500	1. 008	. 428	Air	87	97
2M-4	. 00838	1, 500	1. 008	. 428	Helium	89	97
3M-1	. 01163	1, 362	. 884	. 409	Air	79	88
3M-2	. 01163	1, 000	. 655	. 414	Helium	59	65
3M-3	. 01163	1, 000	. 655	. 414	Air	58	65
4M-1	. 00658	1, 000	. 665	. 422	do	59	65
4M-2	. 00658	1, 972	1. 290	. 410	do	116	128
			4-inch tube				
5M-1	. 00658	2, 975	. 761	. 406	do	75	75
6M'-1	. 01346	2, 223	. 675	. 498	do	58	56

TABLE 19.—*Composition of mixed sands*

Mixture	Weight fraction X retained by sieve range	Sieve range	d_p, inch	d_pX	Calculated D_p, inch
1M	0. 50	0. 0116–0. 0097	0. 01062	0. 00531	
	. 50	. 0097– . 0069	. 00818	. 00409	0. 00940
2M	. 333	. 0116– . 0097	. 01062	. 00354	
	. 333	. 0097– . 0069	. 00818	. 00273	
	. 333	. 0069– . 0058	. 00632	. 00211	. 00838
3M	. 25	. 0164– . 0138	. 01505	. 00376	
	. 25	. 0138– . 0116	. 01268	. 00317	
	. 25	. 0116– . 0097	. 01062	. 00266	
	. 25	. 0097– . 0069	. 00818	. 00204	. 01163
4M and 5M	. 20	. 0116– . 0097	. 01062	. 00212	
	. 20	. 0097– . 0069	. 00818	. 00164	
	. 20	. 0069– . 0058	. 00632	. 00126	
	. 20	. 0058– . 0041	. 00488	. 00098	. 00658
	. 20	. 0035– . 0024	. 00290	. 00058	
6M'	. 25	. 0195– . 0164	. 01790	. 00448	
	. 25	. 0164– . 0138	. 01505	. 00376	
	. 25	. 0138– . 0116	. 01268	. 00318	
	. 25	. 0097– . 0069	. 00818	. 00204	. 01346

Tables 15 to 19 refer to data observed with round and sharp sands during fluidization runs. The gases were passed upward through columns of the various sands. The range of flows during these experiments was wide enough to expand and fluidize the beds. However, for the purpose of pressure-drop correlations through nonfluidizing beds, flow rates up to a certain limiting value (G_{mf}) only should be considered. The significance of the concept G_{mf} will be discussed in greater detail in connection with fluidization. The equipment for these tests is illustrated in figure 51.

CORRELATION OF RESULTS

Figure 29 shows Δp (lb. ft.$^{-2}$ ft.$^{-1}$) corrected to 40-percent voids in relation to the modified Reynolds number. Logarithmic coordinates were used, and the data refer to the sands mentioned in table 13; the correction to the

standard voidage was made by using the relation

$$\Delta p \propto \frac{(1-\delta)^2}{\delta^3},$$

and the value of this relation can be seen from the results obtained. Run a in figure 29, for instance, was made with the same sand compacted to a voidage of 41.0 percent for one experiment and 35.4 percent for another. A decrease in voids from 41.0 to 35.4 percent will almost double the pressure drop; however, by applying the above relation, good agreement between the loosely and densely packed bed runs resulted. The slope of all the lines is (+1) a characteristic of viscous flow.

In figure 30, log Δp has been shown in relation to

$$\log\left(\frac{D_p G}{\mu}\right).$$

The curvature of the lines indicates that the flow was intermediate between the turbulent and viscous range. Figures 31 to 33, showing data originally collected in connection with fluidization, are susceptible to a pressure-drop analysis as long as no bed expansion is experienced. Proportional coordinates were used, and the slope was found equal to unity, an indication of viscous flow. Figure 34 shows data observed with mixtures of sand; the composition of the mixture is given in table 18. As indicated earlier for turbulent flow, the composite diameter of a mixture of sand was calculated by

$$D_p = \sum_{z=1}^{z=z} (X d_p)_z. \qquad (39)$$

Modified friction factors calculated from all the data have been plotted in figure 35, which also incorporates the data of figures 10 and 14. Considering the viscous range only, it appears that the friction factors originating from glass spheres and lead shot are the lowest. By incorporating proper shape factors into the

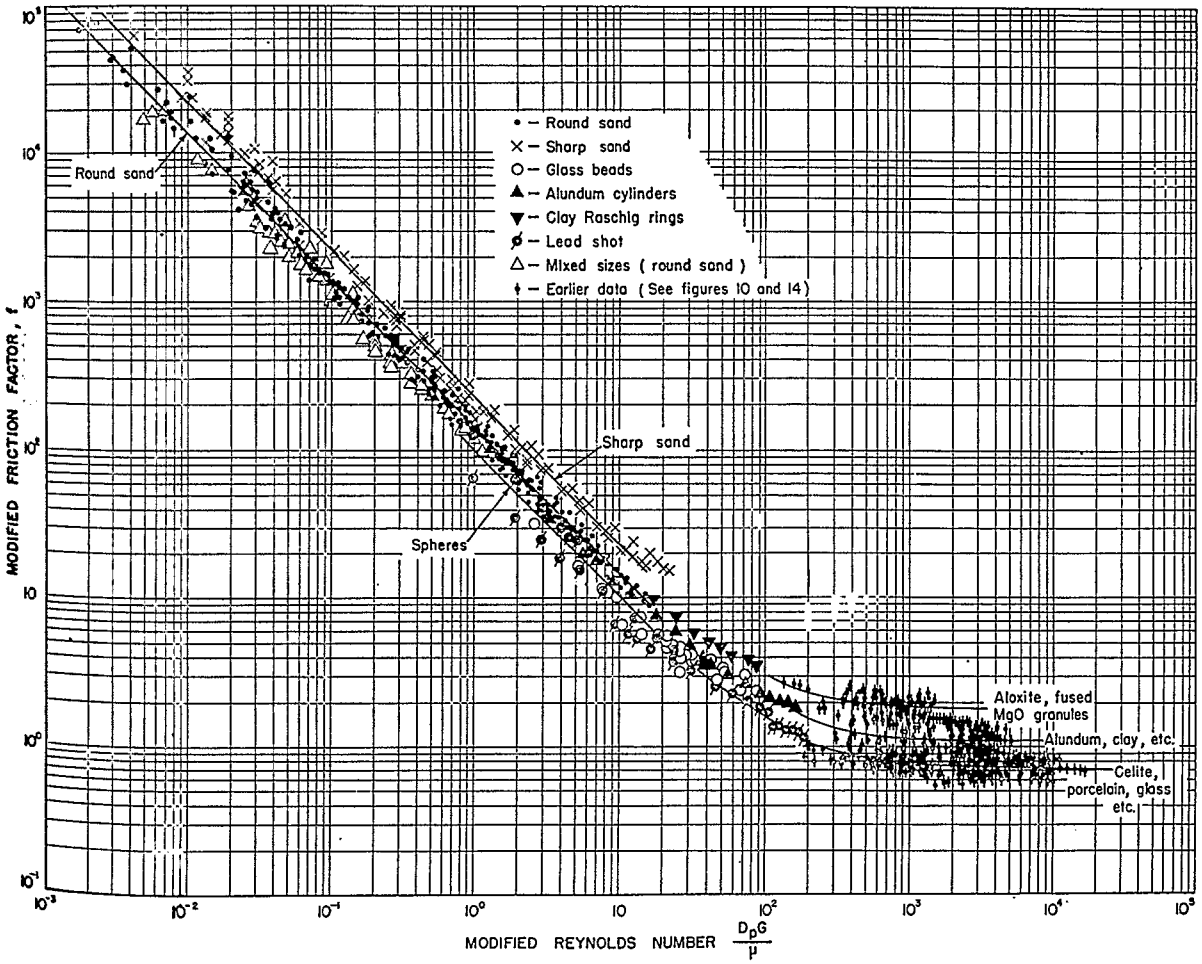

FIGURE 35.—MODIFIED FRICTION FACTORS vs. MODIFIED REYNOLDS NUMBER.

Raschig-ring and Alundum-cylinder data, the line for these particles merges into the line pertaining to smooth spheres. This indicates that the relation $\Delta p, \propto \lambda^2$ is valid for the viscous range and also that surface roughness has no effect upon flow in the viscous range.

Comparisons of friction factors are now possible for the various sands. Thus, at

$$\frac{D_p G}{\mu}=1,$$

for spheres, round sand, and sharp sand, $f=100$, 135, and 225, respectively, permitting calculation of shape factors. Thus, for spheres, $\lambda^2=1.00$ and $\lambda=1.00$; round sand,

$$\lambda^2=\frac{135}{100}$$

and $\lambda=1.16$; and sharp sand,

$$\lambda^2=\frac{225}{100}$$

and $\lambda=1.50$. The friction-factor equation is now readily obtained. From inspection

$$f=100\left(\frac{D_p G}{\mu}\right)^{-1}. \qquad (38a)$$

Substituting (38a) into (37) and using the relation $\Delta p \propto \lambda^2$ results in

$$\Delta pL=\Delta P=\frac{200 G\mu L\lambda^2(1-\delta)^2}{D_p{}^2\rho g_c\delta^3}. \qquad (40)$$

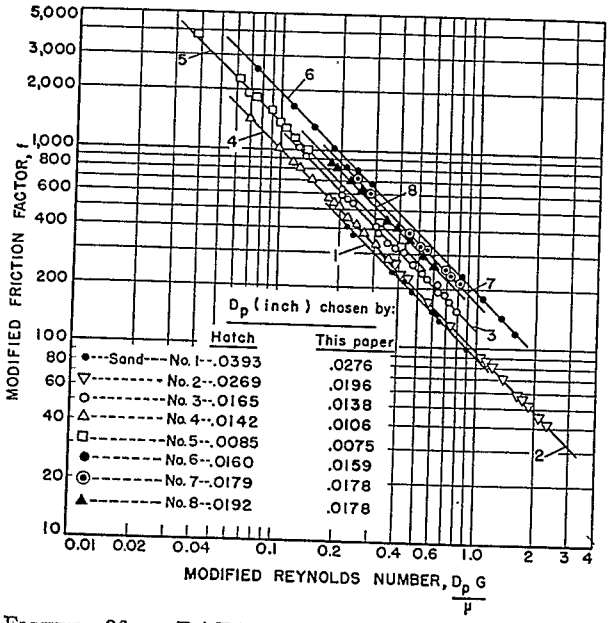

FIGURE 36. — DATA ON FLOW OF WATER THROUGH SANDS, OBSERVED BY HATCH AND CORRELATED BY MEANS OF EQUATION 40.

Figure 36 reports friction factors of the data of Hatch,[33] observed during flow of water through columns filled with various types of sand. Although no shape factors of the individual sands were indicated, Hatch pointed out in his paper that all the materials were very rounded. Comparison of figure 36 with figure 35 emphasizes that essential agreement between water- and gas-flow data exists. Most of the sands investigated by Hatch were mixtures, and failure to reduce all the data into one single line by the correlations advanced in this paper probably is a result of the choice of particle diameter. The relatively smaller deviations in the experimental constant shown in the paper by Hatch indicate that his improved correlation stems from particle diameters that were measured rather than defined by equation (39). It is felt, however, that although equation (39) gives somewhat less accurate results it is sufficiently precise for most engineering work.

COMPARISON OF TOWER PACKINGS IN VISCOUS FLOW

Consideration of equation (40) shows that under laminar flow conditions the bed-characterization factor, β_l, equals

$$\frac{(1-\delta)^2\lambda^2}{\delta^3 D_p{}^2}.$$

On the basis of the earlier turbulent flow conditions and the total available packing area, saddles were believed to be superior to Raschig

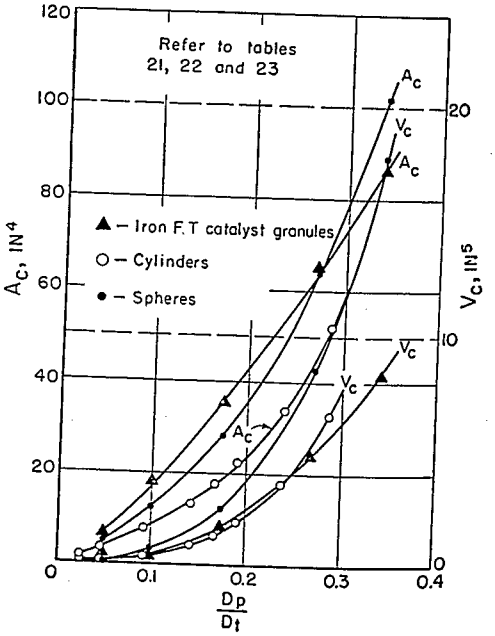

FIGURE 37.—VOLUME AND AREA CHARACTERISTICS FOR VARIOUS TOWER PACKINGS SUBJECT TO LAMINAR FLOW.

[33] Work cited in footnote 37, p. 6.

or Lessing rings. Examination of the calculated data of tables 20 to 23 indicates that (for smaller sizes) saddles are superior to rings if the comparison is made on the basis of surface area. If total volume is the important factor, Raschig rings are the most favorable packing, just as in turbulent flow. Tables 21–23, pertaining to cylinders, spheres, and granules under laminar flow conditions, show that on the basis of area the granules are the most desirable material. The data are also plotted in figure 37 which is analogous to figure 28 pertaining to turbulent flow. Although bed-characterization factors based on laminar flow lead to the same conclusions as those based on turbulent flow, as far as merits of individual packings are concerned, the relative packing efficiencies seem considerably different for the individual shapes involved here. The evaluation of packings on the basis of the concepts introduced here is new, and the ultimate value of the suggested analysis must finally be judged on the basis of more specifically planned experimental studies.

TABLE 20.—*Bed-characterization data for Raschig rings, Berl saddles, and Lessing rings (laminar flow)*

Nominal size, inches	β_l, in.$^{-2}$	A_c, in.^{4}	V_c, in.^{5}
Raschig rings:			
¼	79. 0	315	8. 25
½	16. 5	785	38. 5
1	2. 02	3, 256	214
1 [1]	2. 43	2, 800	199
1½	. 78	5, 230	554
Berl saddles:			
¼	82. 5	377	6. 91
½	20. 8	848	26. 1
1	3. 69	2, 378	114
1½	1. 48	3, 998	274
Lessing rings:			
1	3. 14	2, 480	147
1¼	2. 30	2, 608	223
1½	1. 44	3, 150	377
2	. 621	5, 840	702

[1] Values estimated from void data for cylinders from fig. 25.

TABLE 21.—*Calculated bed-characterization data in laminar flow for cylinders packed 1 foot high in a 3-inch-diameter vessel*

D_p, inch	β_l, in.$^{-2}$	V_c, in.^{5}	A_c, in.^{4}
0.0715	3, 628	0. 0158	1. 53
.143	800	. 0711	3. 42
.286	177	. 316	7. 62
.429	62. 7	. 866	13. 2
.5005	41. 6	1. 28	17. 6
.572	27. 8	1. 90	22. 4
.715	14. 4	3. 53	33. 9
.858	7. 40	6. 53	52. 1

TABLE 22.—*Calculated bed characterization data in laminar flow for spheres, packed 1 foot high in a 3-inch-diameter vessel*

D_p, inches	β_l, in.$^{-2}$	V_c, in.^{5}	A_c, in.^{4}
0.15	465	0. 120	4. 79
.30	88. 7	. 607	12. 15
.525	20. 4	2. 49	28. 4
.81	5. 54	8. 56	63. 8
1.02	2. 53	17. 8	104
1.26	1. 01	42. 6	208
1.44	. 656	59. 9	248

TABLE 23.—*Calculated bed-characterization data in laminar flow for magnetite granules packed 1 foot high in a 3-inch-diameter vessel*

D_p, inches	β_l, in.$^{-2}$	V_c, in.^{5}	A_c, in.^{4}
0.15	480	0. 099	6. 82
.30	84	. 527	18. 3
.525	23. 9	1. 81	35. 6
.81	8. 43	4. 94	63. 7
1.02	4. 85	8. 47	86. 2

COMPARISON OF VARIOUS CORRELATIONS

A comparison of calculated pressure drops according to various investigators [34] is shown in table 24. The analysis pertains to flow of air through a 1-inch-diameter tube. Bed voidages were calculated by using figure 25.

The correlation, according to Chilton and Colburn,[35] suggests very high values for conditions in the turbulent-flow ranges; for laminar flow, on the other hand, the proposed values are the lowest. It is probable that these deviations arise from the fact that the Chilton-Colburn correlation does not make sufficient allowance for the shape of the particles and the voidage in the bed. Agreement between the Carman [36] correlation and the equation proposed in this paper is satisfactory. The Carman equation predicts slightly higher values for the turbulent flow range and for spheres. This may possibly be a result of the fact that Carman considered surface roughness of little importance. The agreement of values proposed by the correlation of Happel [37] with those of Carman and this paper is remarkable, especially since the Happel equation does not specifically account for the effect of particle shape. The Brownell and Katz [38] correlation suggests

[34] See references and footnotes in table 24.
[35] Work cited in footnote 19, p. 4.
[36] Work cited in footnote 36, p. 5.
[37] Work cited in footnote 24, p. 5.
[38] Work cited in footnote 39, p. 6.

unusually low values for flow through ring packings. This is believed to be primarily a result of the voidage function that these investigators used in their correlation. Similar reasoning seems to explain the considerably higher values suggested by the Oman and Watson [39] formula for flow through high-voidage ring packings.

TABLE 24.—*Calculated pressure drops according to various investigators*

Reference	Pressure drop per unit packed height, $\frac{\Delta P}{L}$ (pounds per square foot per foot), for flow of air at 70° F. through a 1-inch tube packed with—		
	Spheres, $D_p=0.25$ in., $\lambda=1.0$, $\delta=0.431$, and $Re=1000$	Smooth rings, ⅜-in. × ⅜-in. × ¼-in., $\lambda=2.18$, $\delta=0.732$, $D_p=0.353$ in., and $Re=1000$	Smooth rings, ⅜-in. × ⅜-in. × ¼-in., $\lambda=2.18$, $\delta=0.732$, $D_p=0.353$ in. and $Re=1$
Chilton and Colburn [a]	153	29. 3	0. 000106
Carman [b]	107	6. 76	. 000373
Oman and Watson [c]	100	14. 9	
Brownell and Katz [d]	68. 8	. 73	. 000234
Authors	81. 6	6. 75	. 000414
Happel [e]	124	5. 45	. 000256
Uchida and Fujita [f]		17. 0	. 000679

[a] Work cited in footnote 19, p. 4.
[b] Work cited in footnote 36, p. 5.
[c] Work cited in footnote 38, p. 6.
[d] Work cited in footnote 39, p. 6.
[e] Work cited in footnote 24, p. 5.
[f] Work cited in footnotes 13 and 14, p. 4.

Some of Happel's data have been recalculated, and friction-factor plots are shown in figures 38 and 39 according to Happel's correlation and equation 41. Although it appears that the equation may be used to predict pressure drop through moving beds when the gas velocity relative to the moving bed is used, the original correlation as proposed by Happel seems to fit the data somewhat better.

NOMOGRAPH

To aid in the rapid solution of equation 40 for any one of the variables when the others are known, the nomograph of figure 40 has been prepared. Estimation of the necessary quantities, such as shape factors and voids, has been covered in previous sections. If particle diameter is the variable sought, the nomogram is of special value because it permits a rapid trial and error solution for values of D_p and δ that are consistent with some established relationship, such as figure 25 or 94.

In using figure 40, it is necessary only to decide on which axis the unknown value will be found and then to follow the order given in the key of the figure to arrive at that axis as the last point. To increase the range of variables without unduly compressing the scales, constants X and Y are used as multipliers as indicated in the figure. Any values of X and Y may be chosen that will keep the values of Xu, Yu, and $XY\Delta P/L$ on the scale; generally, multiples of 10 will be found most convenient.

[39] Work cited in footnote 38, p. 6.

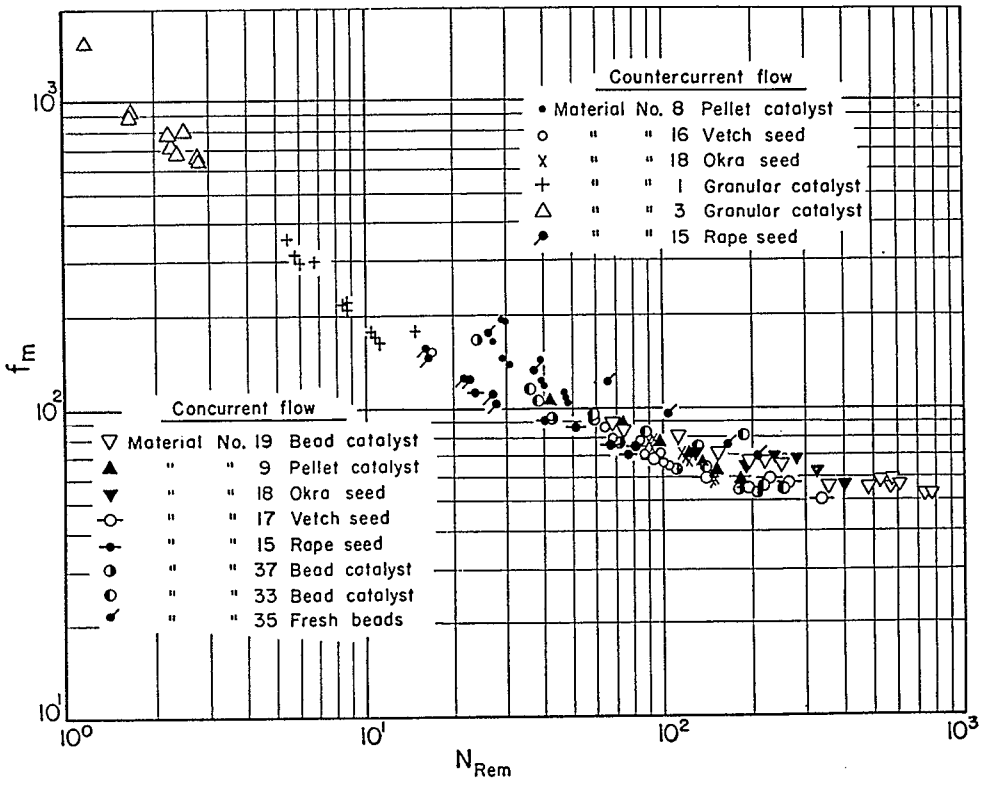

FIGURE 38.—FLOW THROUGH MOVING BEDS; DATA AND CORRELATION OF HAPPEL.

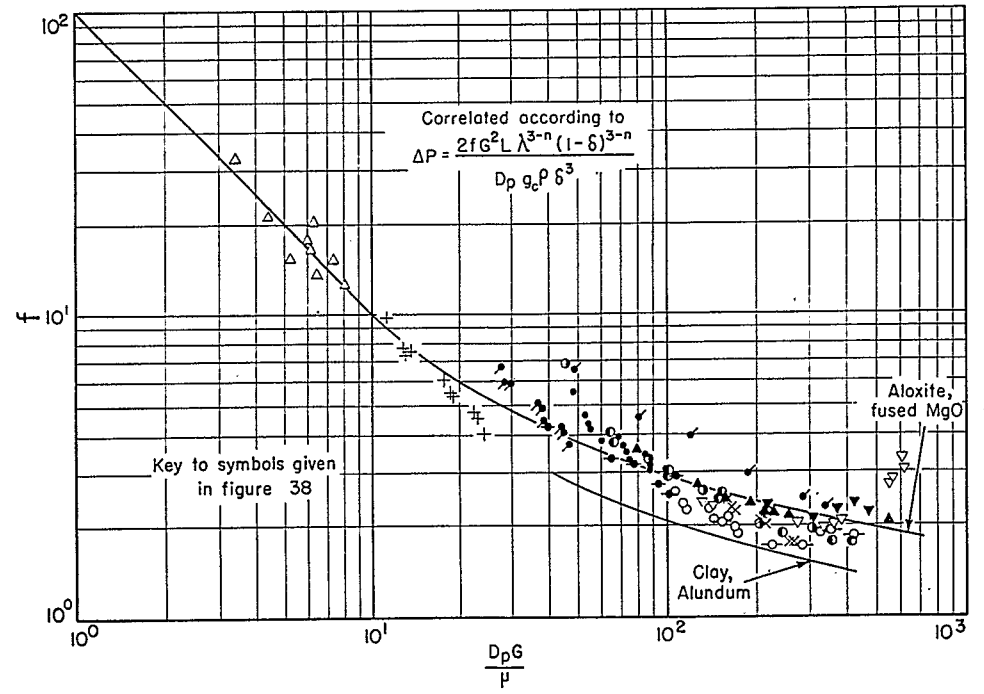

FIGURE 39.—HAPPEL'S DATA CORRELATED ACCORDING TO EQUATION 41.